THE SYNTHESIS OF PBS NANOCRYSTAL AND THEIR SELF-ASSEMBLY INTO COMPLEX NANOWIRE AND NANOCUBE STRUCTURE

by

Fan Xu

A thesis submitted to the Faculty of the University of Delaware in partial fulfillment of the requirements for the degree of Master of Science in Electrical and Computer Engineering

Spring 2011

THE SYNTHESIS OF PBS NANOCRYSTAL AND THEIR ASSEMBLY INTO COMPLEX NANOWIRE AND NANOCUBE STRUCTURE

by
Fan Xu

Approved: _____
Sylvain G. Cloutier, Ph.D.
Professor in charge of thesis on behalf of the Advisory Committee

Approved: _____
Kenneth E. Barner, Ph.D.
Chair of the Department of Electrical and Computer Engineering

Approved: _____
Michael J. Chajes, Ph.D.
Dean of the College of Engineering

Approved: _____
Charles G. Riordan, Ph.D.
Vice Provost for Graduate and Professional Education

ACKNOWLEDGMENTS

I wish to thank my excellent adviser Dr. Sylvain G Cloutier, for his help and guidance in my research.

I must also thank my classmates, Xin Ma, Felipe Gerlein, and Latha for the valuable discussion and help.

I must also thank my family, for their selfless love and support.

TABLE OF CONTENTS

LIST OF FIGURES

ABSTRACT

For the last 50 years, bulk lead-chalcogenide semiconductors have been key materials for infrared light sources and lasers, photodetectors and high-performance thermoelectrics. Meanwhile, the colloidal synthesis of chalcogenide semiconductor nanocrystals has provided a new pathway to producing optoelectronic materials with unique physical properties at low cost, including lead-chalcogenide nanocrystals.

In this thesis, we synthesized various sizes of lead salt nancrystals that exhibit remarkable photoluminescence efficiencies across the near infrared region at room-temperature, which can be appealing active material for light emitting devices, photovoltaic devices, and bio-imaging.

Meanwhile, we developed the catalyst-free self-attachment of PbS nanowires in hot colloidal solution using a combination of multiple surfactants. We demonstrate the controllable self-attachment of star-shaped nanocrystals can lead to radically-branched nanowires while the assembly of octahedral nanocrystals leads to zigzag nanowires. The synthesized nanowires exhibit strong position dependent quantum confinement, which occurs at the side arms and high faceted edges of the nanowires. Those novel structures give rise to the appealing optical properties of the nanowires, with strong photoluminescence in the near infrared region.

Chapter 1

INTRODUCTION

1.1 Context

Colloidal nanocrystals of inorganic semiconductors have been demonstrated with exceptional opto-electronic properties since their first successful synthesis in 1983 [1,2]. Their high absorption cross-section offers promising performance in photo detectors and solar cells [3,4,5], while their narrow photoluminescence spectra tunable across the visible and near infrared region enable it to be an ideal material for light emitting devices and bio-imaging[6,7,8]. Most importantly, compared with conventional epitaxially-grown semiconductor, the solution processability of colloidal nanocrystals allows low cost, large areas, and physical flexible device integration with various platforms, including silicon electronics.

Integrating light-emitting devices capable of efficient operation at telecommunication wavelengths and under electrical injection on silicon chip to realize optical interconnects constitutes an important technological challenge. The silicon lasers based on Raman gain is unable to realize electrical injection [9], while the traditionally compound semiconductor based electrically injected laser is incompatible to integrate on silicon. Indeed, polymer-based light emitting diodes

currently offer great promises for the visible, their potential for operation in the near-infrared remains limited [10].

The colloidal synthesis of semiconductor nanocrystals with high quantum efficiency and tunable emission across the near infrared region enabled a promising approach toward highly efficient infrared electroluminescence and low-cost integration on silicon [11]. To date, a 1.53 μm PbS laser has been realized through the capillary cavity optically through optical pumping [12]. The near-infrared electroluminescence has been demonstrated with an external quantum efficiency of 1.15% [13], while an external quantum efficiency of larger than 2% can be realized in visible electroluminescence diodes [14].

1.2 PbS Nanocrystals

Semiconductor nanocrystals are systems typically consisting of discrete semiconductor particles with diameters on the order of 20 to 200 Å, the energy levels of which is determined by quantum confinement rather than by the inherent properties of the corresponding bulk material. Quantum confinement can occur when the nanocrystal size is smaller than the bulk exciton Bohr radius, $a_B = k\pi h^2/\mu e^2$, where k is the dielectric constant of the material and μ is a bulk exciton reduced mass.

Bulk lead sulfide (PbS) is a π-π semiconductor with a 0.41 eV bandgap at room temperature. Owing to similar effective masses for electrons and holes and a large Bohr radius of 18 nm, PbS nanostructures can strongly and symmetrically confine electrons and holes, and the bandgap emission can be tuned across the near infrared region.

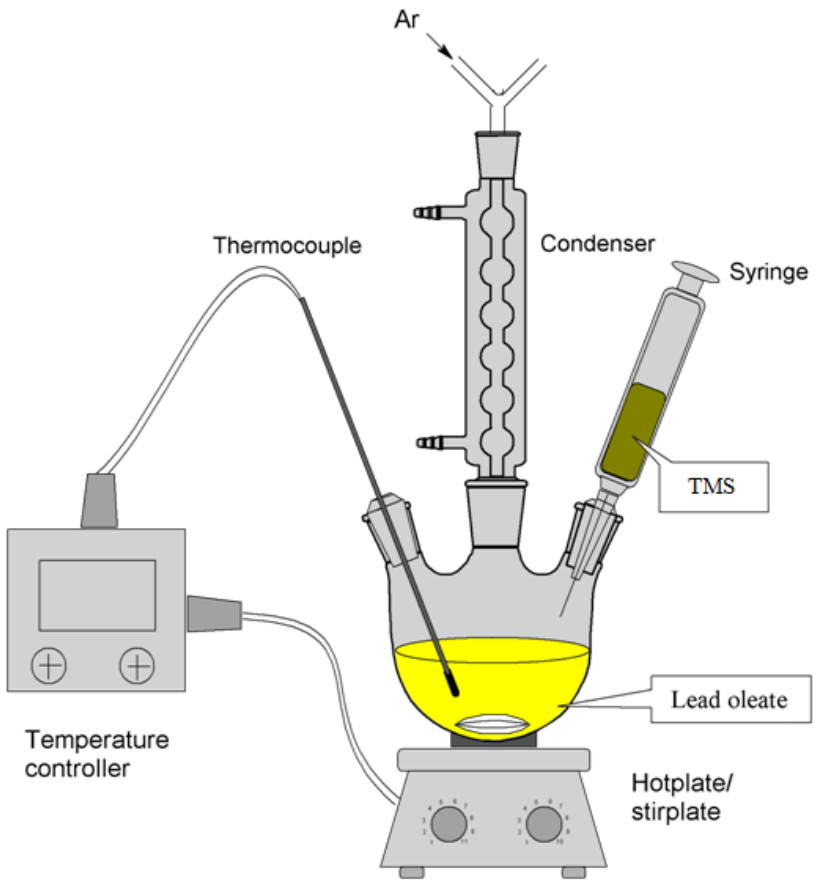

Figure 1.1: Schematic of the nanocrystal synthesis using the three neck flask.

Colloidal PbS nanocrystals can be prepared using the organometallic route with suitable precursors in the configuration shown in the figure above. Organometallic precursors are injected to the hot mixture of organic molecules to generate active monomers in high temperature solvent [15]. The monomers in the solution can form nucleates and grow uniformly into nanocrystals. The nanocrystal growth can be stopped by quenching the reaction with certain solvent or allow it to cool down to room temperature slowly. The nanocrystal size and morphology can be controlled by the concentration ratio among the precursors and surfactants, as well as growth time and temperature. The synthesized nanocrystals are capped with long insulating oleic acid to prevent aggregation, thus ligand exchange must be conducted before the nanocrystal device fabrication.

1.3 Applications of PbS Nanocrystals

1.3.1 Multiple Exciton Generation

PbS nanocrystals have attracted significant interest in the last five years as a way to convert more efficiently high-energy photon, by creating multiple electron-hole pair, instead of losing the extra energy to thermalization [4]. The formation of multiple electron-hole pairs per phonon absorbed in photoexcited semiconductor is a process typically explained by impact ionization when an electron and hole with kinetic energy greater than the semiconductor band gap produces one or more additional excitons. Using PbS nanocrystal-based devices, it was shown that electron-hole pairs generated

per photon can be as high as 2.4 [16]. Using this effect, absorbed phonon to current efficiencies larger than unities has been proved in the photovoltaic device [17].

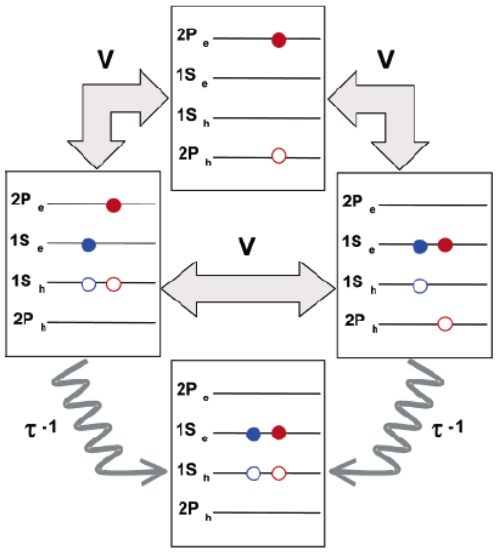

Figure 1.2: Photoexcitation at 3 E_g creates a 2 P_e-2P_h exciton state [4] ©2005 ACS

1.3.2 Hot-Electron Transfer

Hot-Electron Transfer consists of lead-salt nanostructures' ability to very-efficiently pass hot-electrons to wider bandgap semiconductors [18], which also offers great potential for photovoltaic devices. The quasi-continuous conduction and valence energy bands of the bulk semiconductors separated into discrete energy level in nanocrystals, creating a "phonon bottleneck" in which the hot carrier relaxation is the only possible path. While at the interface, highly crystalline wide band gap TiO2 is

used as the electron acceptors, allows the fast hot electron transfer from the nanocrystals to TiO2. The depleted PbS colloidal quantum dot and TiO2 heterojunction solar cell has demonstrated a power converting efficiency of 5.1%.

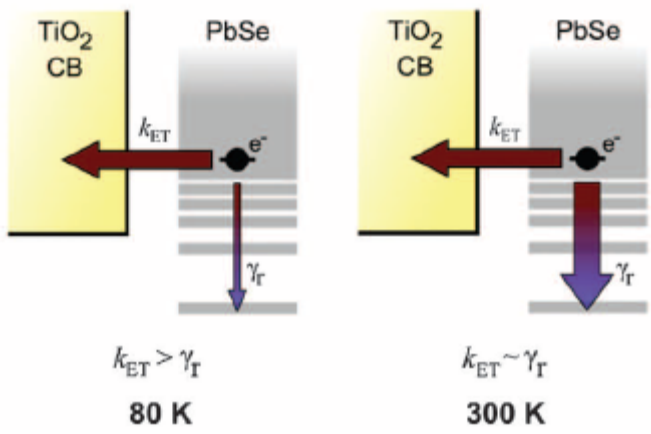

Figure 1.3: Illustration of competing pathways of interfacial electron transfer and intra quantum dot relaxation [18]. ©2010 AAAS

1.3.3 Hybrid Polymer/ QD NIR Light Emitting Devices

Although low-cost molecular and polymeric organics are promising candidates for light emission in the visible range, it remains difficult to extend its optical active region to the NIR owing to the fundamental properties of delocalized π system.

The colloidal synthesis of semiconductor nanocrystals with high luminescence efficiency and narrow spectral emission in the near infrared region enabled a

promising approach toward low-cost and highly efficient infrared electroluminescence [7]. The nanocrystals with tunable bandgap can be achieved by choosing the appropriate size, while solution processability allows the low cost integration onto a variety of substrate and physical flexibility. The incorporation of nanocrystals within the organic polymer based light emitting devices can directly extend the emission to the near infrared.

Electroluminescence spectra of single layer devices based on the mixtures of PbS nanocrystals with MEH-PPV or CN-PPV was demonstrated to be tunable across the range of 1000 to 1600 nm [7,19]. The EL intensity of the PbS nanocrystals capped with octylamine (8 carbon atoms in the chain) was much higher than those capped with oleic acid (18 carbon atoms in the chain), which was explained by the suppression of either Förster energy transfer or direct carrier transfer from the host polymer to the nanocrystal in the case of longer ligand. The Förster energy transfer is a long-range resonant process resulting from dipole-dipole interaction between donor and acceptor molecules, and during this process the energy released from the recombination of the donor (polymer host) is non-radiatively transferred and used to create an exciton on the acceptor (PbS nanocrystal).

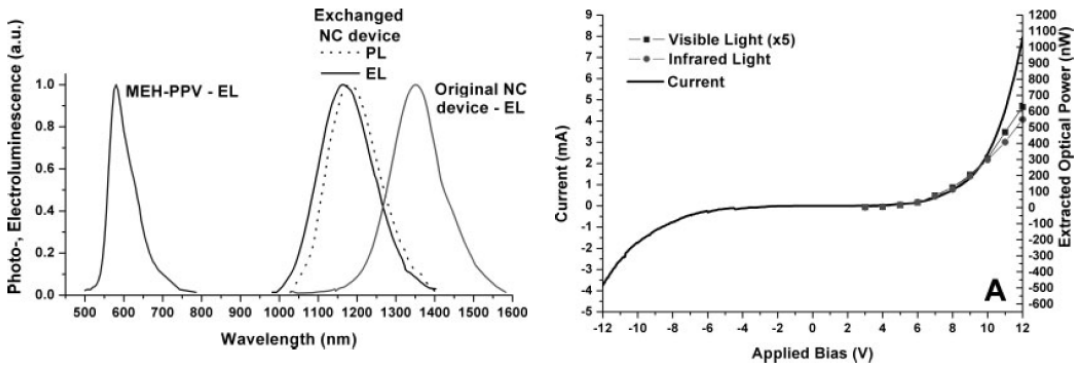

Figure 1.4: (a) The spectral response of the hydrid electroluminescencent devices (b) A typical L-I-V characteristics of a polymer/nanocrystal Mg cathode device [19]. ©2005 WILEY

In a typical polymer-nanocrystal hybrid electroluminescent device, the efficiency is limited owing to the low carrier injection efficiency, the low conductivity of the host polymer, the energy transfer process from the polymer to the QDs, as well as the radiative and non-radiative recombination of excitons prior to energy transfer. As shown in the figure 1.4, the host polymer also contributes a considerably portion of electroluminescence at the visible.

The two key factors to high efficiency and lower operating-voltage hybrid Organic/ QD light emitting devices can be summarized as below:

1. **The Quantum Efficiency of the Nanocrystals**, or the photons generated per exciton generated inside the nanocrystals. This depends mostly on the crystalline perfection and surface passivation of the nanocrystal adopted in the devices.

2. **Exciton Generation Efficiency in the Nanocrystals**, or the excitons generated in the active nanocrystal per carrier injected. This is influenced by the resonant exciton energy transfer from the host polymer to the nanocrystal, and through direct charge injection to the nanocrystal via tunnelling, which depends exponentially on the barrier thickness and thus the ligand length. Meanwhile, keeping the injected carriers in the active region by introducing an electron-block and hole-blocking layers in the devices can retain the carriers in the active region.

Therefore, we believe the realization of the direct injection of carriers into the highly luminescence QDs in the devices could dramatically improve the carrier injection efficiency of the devices.

1.4 Thesis Goals and Organization

In this thesis, we focused on the colloidal synthesis of infrared-acvtive PbS nanocrystals of various shapes and morphology, with emphasises on its opto-electronic properties, and the applications devices in electroluminescence devices. The following fundamental questions are discussed in the thesis:

In chapter 2, a qualitative analysis on the size and shape dependent quantum confinement based on the effective mass approximation and a hyperbolic model are presented, explaining the size tunable photoluminescence of PbS nanocrystals, while the exciton and charge carrier transfer mechanisms in the PbS nanocrystal solid are

discussed as well. In chapter 3, synthetic strategies for the preparation of colloidal nanocrystals are presented. While in chapter 4, the details of PbS nanocrystal synthesis are presented, the nanocrystal size and thus the optical properties of the nanocrystals can be well controlled via adjusting the reaction parameters. We studied the photo stability of the nanocrystals in the atmosphere as well as the effect of surface passivation. The self assembly of high-quality, single crystalline cubic structure PbS nanowires of tunable diameter and complex morphologies are examined in chapter 5. The synthesized nanowires exhibit novel optical properties, owing to the strong position dependent quantum confinement that occurs at the side arms and high faceted edges.

Chapter 2

OPTO-ELECTRONIC PROPERTIES OF PBS NANOCRYSTALS

2.1 Introduction

Cooperative interactions between atoms in condensed matter induce the physical properties that are recognized as characteristics of bulk solids. However, nanocrystals are systems consisting of discrete semiconductor particles with diameters shrinking down to the nanoscale range. In this size regime, there materials exhibit properties that can be characteristic of both bulk solids and molecular systems resulting in many unique features which are interesting and important on both a fundamental level and in regard to the development of applications including optical, electronic and structural effects [20].

2.2 Size Dependent Quantum Confinement

The quantum confinement effect can occur once the diameter of the particle is comparable to the wavelength of the electron, which could be either its De Broglie wavelength or mean free path. The quantum confinement of nanocrystal as a particle in a sphere can occur when the size of the sphere is comparable to the excitonic Bohr radius, which is the length scale of an exciton. An exciton is a quasi-particle that forms

when Coulomb-interacting electrons and holes in semiconductors are bounded into pair states.

2.2.1 Particle-in-Sphere, Effective Mass Approximation

Consider an arbitrary particle of mass m_0 inside a spherical potential well of radius a, where:

$$\hat{H}\Psi = \hat{E}\Psi \tag{2.1}$$

$$V(r) = 0, \;\; r < a;$$

$$= \infty, \;\; r > a;$$

The symmetry of this problem yields the eigenfunctions to the Schrödinger equation, which are similar to the atomic like orbital. The eigenfucntions are labelled by quantum numbers *n*, *l* and *m*, and the boundary value problem of the eigenfucntions is:

$$\Phi_{n,l,m}(r,\theta,\emptyset) = C\,\frac{J_l(k_{n,l,r})Y_l^m(\theta,\emptyset)}{r} \tag{2.2}$$

Where *C* is a normalization constant, J_l is the l th order spherical Bessel function, Y_l^m is a spherical harmonic, and $\alpha_{n,l}$ is the nth zero of J_l, and a is the radius of the sphere.

$$E_{n,l} = \frac{\hbar^2 k_{n,l}^2}{2m_0} = \frac{\hbar^2\pi^2\alpha_{n,l}^2}{2m_0 a^2} \tag{2.3}$$

The Hamiltonian for the quantum dots is similar to the particle in a sphere model when taking into account the electron-hole interaction with each other via a shielded Coulomb interaction [21]:

$$\widehat{H} = \frac{-\hbar}{2m_e}\nabla_e^2 \frac{-\hbar^2}{2m_h}\nabla_h^2 + V(r_e, r_h) \tag{2.4}$$

$$V(r_e, r_h) = -\frac{e^2}{\epsilon|r_c - r_h|} + \text{polarization terms} \quad r < a; \tag{2.5}$$

$$V(r_e, r_h) = \infty \quad r > a$$

The same as in bulk semiconductor solid, the atoms in the crystal can be accounted for by introducing Bloch wavefunctions:

$$\Psi(r) = \sum_k C_{n,k}\, u_{n,k}(r) e^{ikr} \tag{2.6}$$

Where the free electron wave is modulated by $C_{n,k}$, the expansion coefficient, which ensures that the sum satisfies the spherical boundary conditions; and $u_{n,k}$, the periodic potential accounting for atoms. If it assumed that the $u_{n,k}$ has a weak dependence on k, then Equation 2.6 can be rewritten as:

$$\Psi(r) = u_{n,0}(r) \sum_k C_{n,k}\, e^{ikr} = u_{n,o}(r) f(r) \tag{2.7}$$

An approximated solution can be obtained by taking the solution for the first excited state of the particle in a spherical problem and assuming that the electron and hole are uncorrelated, then the solution to equation (2.1) can be written as:

$$\Delta E = \frac{\hbar^2 \pi^2 \alpha_{n,l}^2}{2a^2}\left({}^{1}/_{m_e} + {}^{1}/_{m_h}\right) - \frac{1.8e^2}{\epsilon R} + small\ polariztion\ term \tag{2.8}$$

Where ΔE is the energy of the first excited state, the first term is the kinetic energy of the electron and hole which increases as the particle size decreases, the second term is the screened Coulomb interaction which stabilizes the electron-hole pair, and the third term is the polarization energy which is generally small. For the first

three levels, $\alpha_{n,l} = 1(1S), 2.04(1P), 3.36(1D)$. Since the second and third energy levels are significantly higher than the first confined energy level, only the first optical transition is considered here.

2.2.2 Hyperbolic Model

The hyperbolic model is based on the notion that the lowest exciton of the PbS lattice involves a simple electron transfer form S^{2-} to Pb^{2+}, at a cost in the energy equal to the bulk band gap E_g, and the assumption that for purposes of calculating the band gap only two bands are important, namely the highest occupied valence band and the lowest unoccupied conduction band [22].

Now, $\Psi_1(\boldsymbol{r})$ can be is defined as the amplitude of the localized valence band state at the unit cell at **r,** and $\Psi_2(\boldsymbol{r})$ corresponding to the conduction band state. Ψ_1 and Ψ_2 are related by electron transfer between S and Pb, and the Hamiltonian coverts one kind of state to the other, and it can be written as:

$$\mathrm{H}\Psi_1(\mathrm{r})=\mathrm{E}_1\Psi_1(\mathrm{r}) + \sum_{\mathrm{r}'} \mathrm{A}(\mathrm{r}-\mathrm{r}')\Psi_{12}(\mathrm{r}') \tag{2.9}$$

$$\mathrm{H}\Psi_2(\mathrm{r})=\mathrm{E}_2\Psi_2(\mathrm{r}) + \sum_{\mathrm{r}'} \mathrm{B}(\mathrm{r}-\mathrm{r}')\Psi_{21}(\mathrm{r}')$$

Where function A and B describe transfer to neighbouring sites, and the local energies E_1 and E_2 are related by:

$$E_g = \mathrm{E}_1 - \mathrm{E}_2 \tag{2.10}$$

The eigenvalues of equation (2.9) can be found by solving the equation:

$$\sum_{r'} C(\mathbf{r} - \mathbf{r}')\Psi_1(r') = \lambda\Psi_1(r) \tag{2.11}$$

And ? is given by the lowest eigenvalue as for the τ point exciton describe by:

$$\lambda = \frac{E_g \hbar^2 \pi^2}{2m^* a^2} \tag{2.12}$$

The ΔE is the difference if the two roots, which give the energy of the first excited state as:

$$\Delta E = (E_g^2 + 4\lambda)^{1/2} = (E_g^2 + \frac{2E_g \hbar^2 \pi^2}{m^* a^2})^{1/2} \tag{2.13}$$

The comparison of the bandgap of PbS nanocrystals as a function of size by effective mass approximation, hyperbolic band model and the experimental data is shown in Figure 2 (b). It is clearly observed that effective mass approximation breaks down as the QDs get smaller, since the assumption that the energy surfaces are parabolic in k is valid only for small k (large diameter). On the other hand, the hyperbolic band model includes the nonparabolicity of the band structure and accurately matches with the experimental results. However, it is incapable of calculating energies of higher excited states because it models only the lowest interband transition as an electron transfer between lead and sulphur.

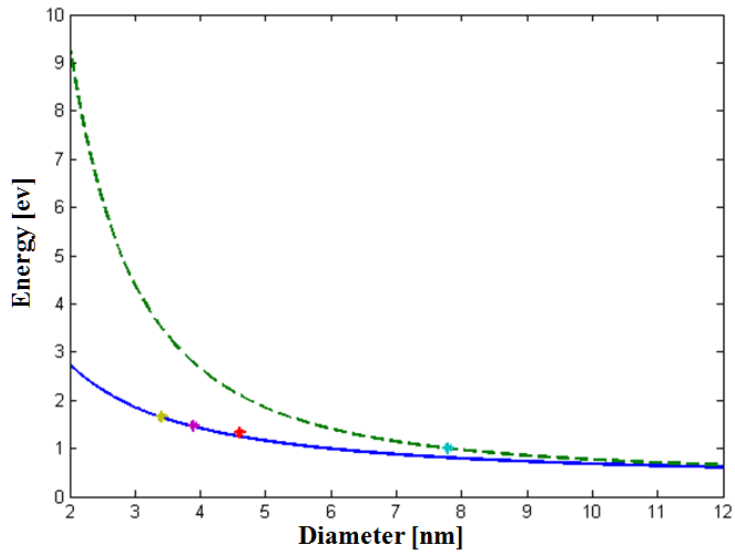

Figure 2.1: Comparison of the bandgap of PbS as a function of particle size calculated with effective mass approximation (dashed line), hyperbolic band model (solid line) and the experimental data (diamonds).

2.3 Shape Dependent Quantum Confinement

Nanocrystals can exhibit interesting size-dependent quantum confinement, as well as the shape dependent quantum confinement. Quantum confinement can occur in all three dimensions, determined by how many dimensions approach the Bohr radius. The varying degrees of confinement have a dramatic influence on the opto-electronic properties of the nanocrystals, as shown in Figure 2.1. In the bulk form, the density of state $\rho(E)$ is proportional to $\sqrt{E}$ given by:

$$\rho(E) = \frac{mK}{\pi^2 \hbar^3} = \frac{m}{\pi^2 \hbar^3}\sqrt{2mE} \tag{2.14}$$

Where K is the wave vector, ρ is the density of states, and E is the energy, $\rho(E)$ rises continuously above the bandgap as the entire range of K space is accessible to the carrier.

If the confinement occurs in one dimension, the structure is referred to quantum well, or a 2D structure as the carrier is free to move and the energy levels remain continuous over the 2 dimension sheet, while the confinement in the other dimension results discrete energy levels [23]. This gives:

$$E_n(k_x, k_y) = \epsilon_n + \frac{\hbar^2 k_x^2}{2m} + \frac{\hbar^2 k_y^2}{2m} \tag{2.15}$$

The discrete energy level along the confined direction gives rise to a step-like density of states as a function of energy as shown in Figure 2.1.

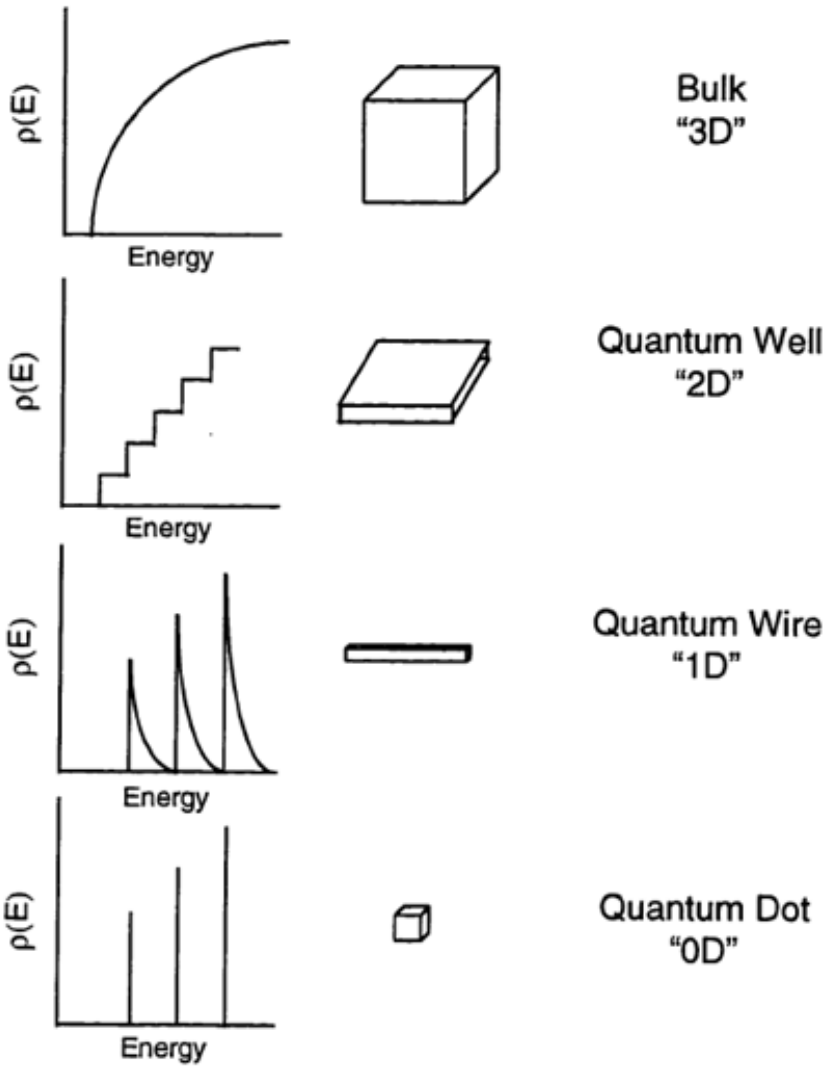

Figure 2.2: Schematic depiction of the density of states and confinement dimensions for bulk material, quantum well, quantum wire, and quantum dot.

Similarly, in a 1D nanowire structure, the carrier is confined by 2 dimensions and is able to move along the axis direction. The energy levels are discrete in two dimensions and the other is continuous. While in a 0D quantum dot, the carrier is

confined in three dimensions and all allowed energies are confined to specific levels resulting a $\delta(E)$ function of the density of states, with large $\rho(E)$ at particular values and zero density of state elsewhere.

2.4 Photoluminescence of PbS Nanocrystals

Photoluminescence quantum efficiency is defined as the ratio of the photons emitted from the nanocrystals over the number of photons absorbed. It depends on the surface and defect states, which provide means for the nonradiative recombination of nanocrystals. Photoluminescence spectra for PbS nanocrystals in solution of various diameter rang from ~3.6 nm to ~7 nm is shown in Figure 2.3 (a), corresponding to the band-edge photoluminescence of from ~0.8 eV to ~1.1 eV. Although PbS nanocrystals with remarkable quantum efficiency of 80% can be synthesized in solution [25], it severely drops in the form of solid nanocrystal thin films, as a result of energy transfer to non-luminescent surface and defect states, as well as charge carrier separation among the neighbouring nanocrystals through tunnelling.

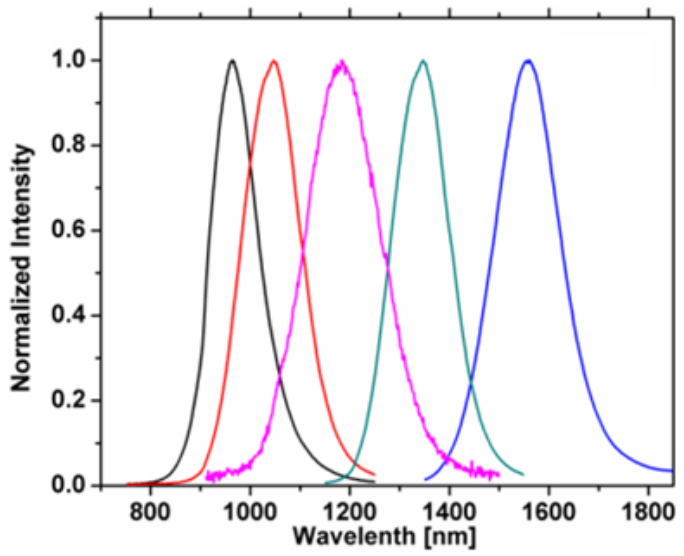

Figure 2.3: Photoluminescence spectra for PbS nanocrystals of various sizes.

2.5 Charge Carrier Coupling in Nanocrystal Solids

In a closely packed nanocrystal solid, the opto-electronic properties depend not only on individual nanocrystal, but equally on the interactions and coupling among proximate nanocrystals. This determines the energy transfer and charge transport characteristic in the nanocrystal film.

2.5.1 Exciton Energy Transfer

The Förster energy transfer is a long range resonant process resulting from dipole-dipole interaction between donor and acceptor molecules, Coherent Förster resonance energy transfer can occur between among nanocrystals of different sizes in

monodisperse or mixed nanocrystals assemblies when dots are in close proximity to each other and when there is sufficient overlap between the donor emission and the acceptor absorption spectra [26]. Here, the smaller nanocrystals with larger bandgap would function as the donor, while larger nanocrystals with smaller bandgap work as the acceptor. Consequently, there will be a constant exciton energy flow from the smaller nanocrystals to larger ones upon excitation, as shown in Figure 2.4. Meanwhile, a considerable portion of the energy will relax to the defect and trap states, and recombinate nonradiatively.

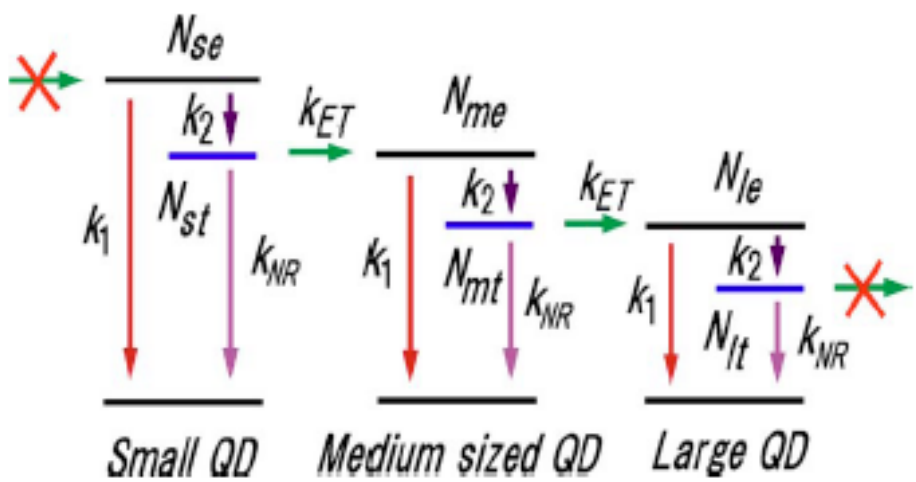

Figure 2.4: The relaxation process of PbS nancrystals in close-packed film. K_1: inter band recombination, K_2: excitons relaxed to the surface states, K_{NR}: Non-radiative recombination, K_{ET}: resonant energy transfer. Nst N_{mt} N_{lt} corresponds to small, medium and large nanocrystals [27]. ©2010 AIP

The Förster energy transfer is typically characterized by the Förster radius R_F, the distance at which a donor exciton is likely to transfer its energy to the acceptor. The Förster radius R_F is given by [28]:

$$R_F^6 = \frac{(9000k^2\ \mathrm{In}10)}{128\pi^5 N*n^4}\int \frac{E_d(\omega)\epsilon_a(\omega)}{\omega^4}d\omega = \frac{(9000k^2\ \mathrm{In}10)}{128\pi^5 N*n^4}\int \frac{E_d(\lambda)\epsilon_a(\lambda)}{\lambda^4}d\lambda \tag{2.16}$$

$$K_{ET} = \frac{\Psi_D}{\tau_D}\left(\frac{R_F}{R}\right)^6 \tag{2.17}$$

In this expression, k^2 is an orientation factor that is assigned the value 2/3, N is Avogadro's number, Ψ_D is the quantum yield of the donor, $E_d(\omega)$ is the normalized donor emission spectrum, $\epsilon_a(\lambda)$ is the molar extinction coefficient of the acceptor, and R is the distance between the donor and acceptor cites. The resonant energy transfer can be extremely efficient when the overlap between the emission spectrum of the donor material and the absorption spectrum of the acceptor material matches well. Murray et. al. have demonstrated an efficiency of energy transfer rate of 94% [26].

2.5.2 Charge Carrier Transfer Via Tunnelling

When the inter-particle coupling is significantly reduced through surface chemistry, the charge transfer among neighbouring could occur via tunnelling [29]. The wavefunction of isolated nanocrystals decays exponentially with distance from the center. The charge transfer rate can be described with the Marcus theory in the case of symmetric reorganization energy and Gibbs free energy, with a simplified rate distance relationship in the form [30]:

$$k_{et} = k_0 \exp(-\beta d) \tag{2.18}$$

Where β is the electron tunnelling constant, and d is the donor-acceptor distance, which is the neighbouring inter nanocrystals distance here, describing the tunnelling of the charge through a potential barrier. The charge transfer through a coherent tunnelling process can efficiently separate the excitons in the nanocrystals at short inter-particle distance.

Typical LED devices require high electronic coupling, thus shorter inter-nanocrystal distance and lower inter nanocrystal barrier, for efficient charge transfer. Meanwhile, nanocrystal materials should be chosen with large exciton binding energy so as to quench the charge carrier separation and allow the dominating radiative recombination.

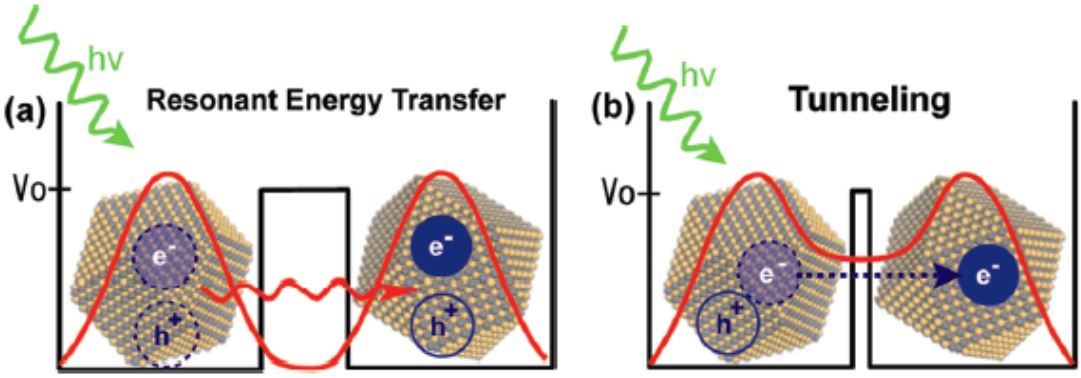

Figure 2.5: Scheme showing long range resonant Förster energy transfer in (a) and charge transfer through tunnelling in (b) [29]. ©2010 ACS

2.6 Conclusion

This chapter discussed the size- and shape-dependent quantum confinement effect, photoluminescence, as well as the exciton and charge-carrier transfer properties of PbS nanocrystals.

The hyperbolic band model accurately predicts the bandgap of PbS nanocrystal as a function of size, while the effective mass approximation breaks down as the size of the nanocrystals goes down. PbS nanocrystals can exhibit appealing quantum efficiency in the solution, while it drops dramatically in a close packed nanocrystal solid when excitons are transfer to the neighbouring non-luminescence nanocrystals via the long range Förster energy transfer. When the nanocrystals are in close approximation, tunnelling can occur and induce the separation of carrier changes. This can significantly improve electronic coupling in the nanocrystal based devices.

Chapter 3

NANOCRYSTAL SYNTHETIC STRATEGIES

3.1 Introduction

As discussed in the last chapter, nanocrystals can exhibit properties that are characteristics of both molecular species and solid-state materials. Colloidal nanocrystals have an inorganic core capped by a layer of surfactants. They can exhibit size tunable band gaps and luminescence energies owing to the quantum confinement effects [1,11]. Preparation of nanocrystals that are uniform in composition, size, shape, internal structure, and surface chemistry is essential to study their physical dependent properties.

3.2 Requirements of Nanocrystals

Before examining reaction precursors and parameters in the nanocrystal synthesis, there are three essential characteristics with regard to the quality of the nanocrystal sample that must be considered. Firstly, the nanocrystal must be highly crystalline, where the constituent atoms in the nanocrystal are arranged in an orderly repeating pattern extending in all three spatial dimensions [31]. The band structure, density of states, quantum confinement and optoelectronic properties of the nanocrystal all

depends on the existence of a periodic lattice structure. If the nanocrystal were poorly crystallized or amorphous, the unique properties of nancroystal will not be expected. Meanwhile, if the nanocrystal contain multiple crystal domains instead of a single crystal domain, the discussion of size dependent quantum confinement effect would be much more difficult and of questionable validity.

The second key factor is the size distribution of the nanocrystals. In the nano-regime where the properties of the nanocrystals exhibit strong size-dependence, it is critical to achieve well defined nanocrystals size distribution. To resolve the absorption and fluorescence features and assign shifts owing to quantum confinement, the inhomogeneous broadening originate from the nanocrystal size distribution must be minimized [11]. Meanwhile, as for the device application, narrow size distribution can improve the uniformity of nanocrystal solid and allows the self assembly of nanocrystals into 2D and 3D superlattices [32,33], it can give rise to sharp light emission in the quantum dot LED devices as well.

The third requirement is that the nanocrystals can form stable solution in common solvents. This ensures that the particles each remain as discrete entities and do not fuse or degrade over time.

3.3 Colloidal Nanocrystal Preparation

The synthesis of colloidal nanocrystals generally includes three parts: precursors, solvents and organic surfactants, which could often serve as solvents as well. To obtain colloidal nanocrystals, a suitable precursor needs to rapidly decompose or react at certain growth temperature in the solvent to yield a chemically active monomer. Meanwhile, the existence of surfactants can modify the growth of the nanocrystals, prevent agglomeration and fusing of particles, and provide solubility to the nanocystals in common solvents.

The formation of nanocrystals involves a discrete nucleation event followed by a rapid growth from monomers and then the slower aging process. In the nucleation step, precursors decompose at relatively high temperature to form a super-saturation of monomers followed by a burst of nucleation of nanocrystals, creating sites where the nanoparticles proceed to grow [31]. A rapid and instantaneous nucleation separated from the growth process is of crucial importance to obtain monodisperse nanocrystals, since all the nucleation sites can undergo the same period of growth in this manner. The best way to achieve instantaneous nucleation is to inject the precursors at high temperature such that nucleation occurs immediately before the nanocrystal growth starts [1]. In contrast, a slow nucleation process results in inhomogeneous nanocrystal growth and give rise to a broad size distribution.

The following growth of highly crystalline semiconductor nanocrystal typically needs a high temperature to allow the rearrangement of atoms and anneal the nanocrystals. During the growth, the surfactants can coordinate or bond to the nanocrystal surface. Indeed, the surfactants must be chosen with a appropriately adhesive energy so that they can attach on and off the growing nanocrystals [31], thus the nanocrystal surfaces are transiently accessible for growth while the entire nanocrystal is still well capped to prevent aggregation.

The surfactants for colloidal synthesis of nanocrystals typically contain an electron-rich donating group such as phosphine, amines, and acids. They behave as Lewis base that coordinates to the acid-like metal of the semiconductor, while the other end of the ligand imparts solubility to nanocrystal by giving the particles a hydrophilic or hydrophobic surface. For example, the alkyl groups of trioctylphosphine capping enable nanocrystals solubility in relatively nonpolar solvents while using ligands such as mercaptobezoic acid result in particles that are soluble in polar solvents like methanol due to more polar functionalities.

3.4 Growth Mechanisms

The growth of nanocrystal start from the super-saturation of monomers followed by a burst of nucleation of nanocrystals in the reaction solution, and the reaction needs to be rapid and complete. These characteristics require colloidal systems using

reagents with low barriers to reaction. For example, in the colloidal synthesis of lead-salt nanocrystals, the most successful PbSe nanocrystal synthesis, $PbC_{17}H_{33}COO_2$ + $[Se(TOP)_3]$ in octadecene or diphenyl ether, provides a ideal combination of instantaneous reaction along with the ability to control the nucleation event [34]. While in the PbS synthesis, owing to the relatively low reactivity of $[S(TOP)_3]$, a much higher reaction temperature above 200 ^oC must be employed. Consequently, a highly active sulfide precursor TMS is often used to replace $[S(TOP)_3]$, and a well controlled nucleation and subsequent growth is achieved [35]. This reaction can even occur at room temperature, giving rise to the ultra-small nanocrystals with large size distribution and a mean diameter smaller than 3 nm, where extremely strong quantum confinement occurs.

Meanwhile, selective nanocrystal growth and the final shape evolution of the nanocrsystals can be well guided by choosing the important parameters in the reaction. The PbS nanocrystals with 1 D, 2D and other more complex morphologies have been obtained [32, 35]. For example, the use of multiple capping agents such as TOP and oleylamine is useful for its ability to generate shape anisotropy in PbS nanocrystals, and also for its intrinsic hexagonal structure. The first critical factor responsible for the shape determination of nanocrystals is the crystallographic phase of the initial nanocrystal seed during the nanocrystal nucleation [36]. Those seeds can have a variety of different crystallographic phase, while the stable phase is highly dependent

on temperature. By adjusting the initial reaction temperature during the nucleation process, the crystalline phase of the seeds can be controlled. For example, the shape of CdSe nanocrystals can be controlled by tuning the reaction temperature. At low temperature, zinc blend tetrahedral seeds with four {111} are formed, while on the other hand, exclusive 1 D CdSe nanorod formation is observed owing to the formation of stable wurtzite phased seeds at high temperature [37].

After the formation of preferred crystalline phase during the initial nucleation stage, the subsequent growth stage governs the final architecture of the nanocrystals through the delicate balance of the kinetic growth and thermodynamic growth regimes [36]. At the high-temperature thermodynamic regime, the reaction is governed by a high flux of thermal energy kT and a low flux of monomer, where the most stable form of nancrystals is formed. On the contrary, the high flux of monomers dominates the growth at the kinetic growth and the anisotropic growth among different crystalline phases is facilitated. Simultaneously, the surface energy of the crystallographic phase is another key parameter that can influence the nanocrystal growth since the kinetic energy barrier is inversely proportional to the surface energy. By choosing the appropriate types and ratios of the surfactants during the nanocrystal growth, the surface energy of each crystalline facet can be well controlled. Finally, the ratio among the molecular precursors can be another critical factor to control the kinetic growth.

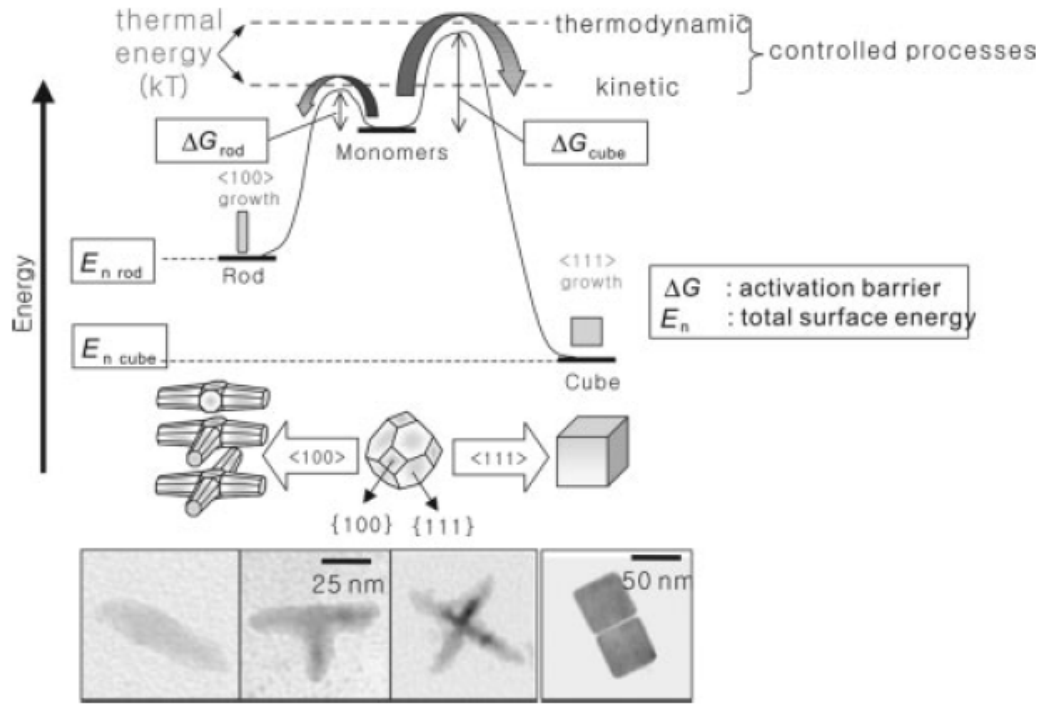

Figure 3.1: Schematic energy diagram of PbS nanocrytsals, their growth modes, and TEM images of resulting shapes of PbS nanocrystals depending on the growth mode [36]. ©2005 WILEY

The shape evolution of PbS nanocrystals provides a good example of such process. Rapid injection of reaction precursors into the hot reaction solution induces the formation of {100} and {111} terminated nanocrystal nucleates [34], and the subsequent growth on these two facets determines the final structure of the nanocrystal. Under high reaction temperature when the thermodynamic energy dominates nanocrystal crystal growth, the most cubic nanocrystal are formed owing to the excess growth of {111} facets. However, in the presence of the capping surfactant

amine which can tightly bind to the {111} surface, the growth on the {111} facets can be significantly suppressed. Consequently, the relatively faster growth of {100} can induce the formation of star shape and octahedral nanocrystals.

3.5 Size Selective Precipitation

If the nanocrystals have a wide size distribution, size selective precipitation techniques can be used to isolate narrower distributions based on the differential solubility of particle sizes. By slowly changing the salvation ability of the solvent system through the incremental addition of a solvent of different polarity, particles will precipitate by size due to the fact that attractive forces such as Van Der Walls forces are size dependent. Other factors such as shape and surface structure also affect precipitation, but if these other factors are similar across the size distribution, size will be the dominant variable controlling the precipitation.

3.6 Conclusion

Strategies to synthesize nanocrystals must seek to ensure the quality of the nancrystals including the formation of discrete nanocrystals with sound crystalline structures, well-resolved size distribution, as well as the solubility in the common solvents. The preparation of colloidal nanocrystals involves the precursors, solvents and organic surfactants. The formation of high quality nanocrystals require precursors decompose to form a super-saturation of monomers followed by an instantaneous

nucleation of nanocrystals, creating sites where the nanoparticles proceed to grow. Finally, the surfactants allow a controllable nanocrystal growth, preventing nanocrystals agglomeration and provide solubility to the nanocrystals in common solvents. The growth proceeds until the reagents are consumed and reaction goes to completion, while the high temperature annealing allows for the good crystallinity of the quantum dots.

Chapter 4

COLLOIDAL SYNTHESIS OF PBS NANOCRYSTALS

4.1 Introduction

Highly luminescent PbS nanocrystals of suitable size for telecommunications have been fabricated. These nanocrystals have sound crystalline structure and are soluble in a variety of organic solvents including hexane, toluene and chloroform. The size distribution of the nanocrystal is narrow, no size selective precipitation of nanocrystals is needed. After the nanocrystal synthesis, the surface of the nanocrystals can be modified with a variety of ligands including amines, thiols, and other phosphines. The optical properties of the nanocrystals, especially the photoluminescence is very sensitive to the surface passivation of the nanocrystals. These colloidal nanocrystal offers the advantages of being solution based, and have been successfully used as the luminescent material in polymer based light-emitting diodes, lasing, optical detection and photovoltaic devices across the near infrared range [6,12,13].

4.2 PbS Nanocrystal Synthesis

PbS quantum dots were prepared in a slight modified method of Hines et al [11].

$$PbO + CH3(CH2)7CH = CH(CH2)7COOH \rightarrow PbC_{17}H_{33}COO_2$$

$$PbC_{17}H_{33}COO_2 + (CH_3)_3SiSSi(CH_3)_3 \rightarrow PbS$$

All the synthesis process is done inside a nitrogen purged glove-box. Lead oxide (2 mmol), Octadecene (10 ml) and Oleic Acid (4 mmol) were first added to a single flask. The mixture was heated under in glove-box at 120 ℃ until the frothing had subsided and all of the lead oxide (lead acetate) had dissolved. The mixture was then kept at the desired temperature between 70℃ ~150℃. Subsequently, Hexamethyldisilathiane (1mmol) solution diluted by ODE (5 ml) was quickly injected into the reaction flask under vigorously stirring. The color of the reaction solution changes from dark blue to red and finally to black rapidly after the injection of sulfur precursor, indicating a rapid nucleation process. The remaining monomer feeds the growth of those nucleate rapidly. The reaction solution was annealed for 1 min, then the hot plate is unplugged and the reaction solution is slowly cooled down to room temperature. The nanocrystals are finally collected by injection of reaction solution into an organic polar solvent such as methanol, acetone or ethanol for centrifuging. The precipitates were dried in vacuum and redispersed in toluene or chloroform. To ensure adequate removal of the reaction solvents, precipitation and redispersion was repeated again. The nanocrystal solution was filtered with 200 nm polytetreafluoroethylene filters before solution ligand exchange and device fabrication.

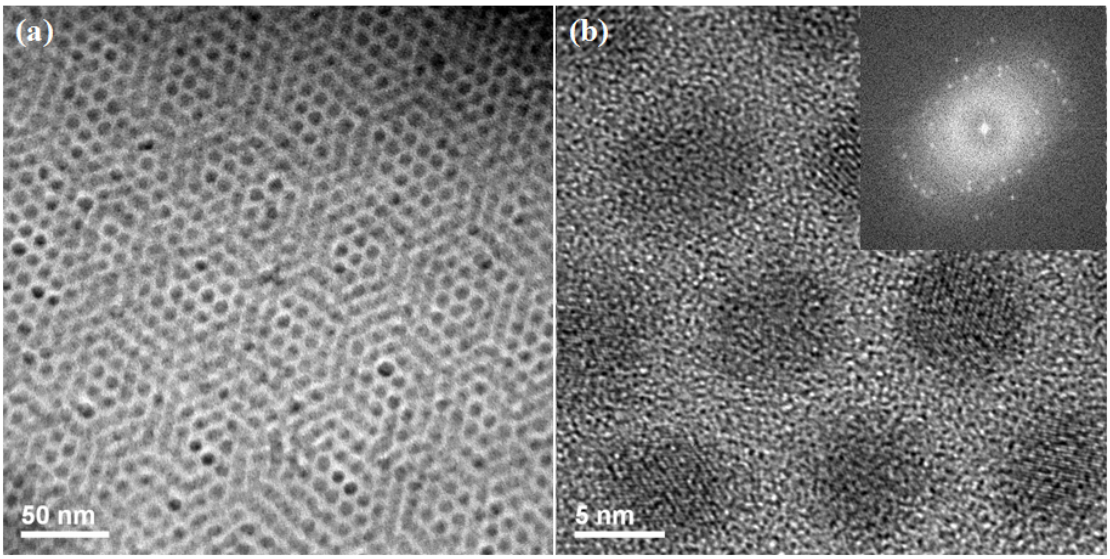

Figure 4.1: TEM (a) and High resolution TEM (b) images of PbS nanocrystal with a mean diameter of ~7 nm and with a photoluminescence peak at 1520 nm. The inset shows the FFT of the HRTEM images.

TEM image of typical PbS nanocrystals with an mean diameter of ~7nm is shown in Figure 4.1 (a), the highly orderly nanocrystal array indicates the uniformity and monodispersity of the as synthesized nanocrystals, while the sound crystalline structure of the nanocrystals is confirmed in the high resolution TEM image in Figure 4 .1 (b).

4.3 Size Control of Nanocrystals

It is of great importance to control the size of the nanocrystal in colloidal synthesis, since the band-gap absorption and luminescence energy of the PbS nanocrystal depends on the size through quantum confinement.

During the synthesis, the nucleation and the growth process of PbS nanocrystals were instantaneously finished after the injection of the sulfur precursor. TEM images combined with the PL measurement shown in Figure 4.2 demonstrate that nanocrystals taken from the reaction at intervals of 1 min, 2 min, 5 min, and 30 min are actually of the same size and band edge emission energy. Therefore, we believe the key to control the size of the QDs lies in the controlled nucleation event. According to the references and the observations in our experiments [11,38,39], there are mainly three factors that influence the growth pattern of the QDs: the injection temperature, the molar ratio among the surfactants and precursors, and the monomer concentration.

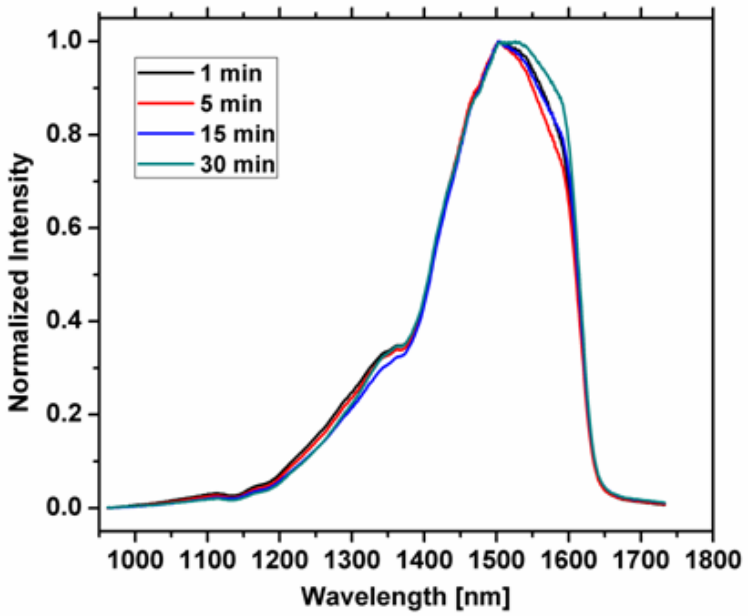

Figure 4.2: Photoluminescence spectrum of PbS nanocrystals taken from the reaction after growth of 1 min, 2 min, 5 min, and 30 min.

Larger nanocrystals synthesized with small fraction of active surface atoms are more thermally stable compared to the smaller nanocrystals. When the reaction is driven by a sufficient supply of thermal energy at high reaction temperature, the more stable large nanocrystals are formed. Secondly, it was found that high OA concentration can lower the monomer reactivity and reduce the nanocrystal nucleation [11]. Therefore, the monomers will feed to the growth of the nanocrystal at high OA concentration, so as to obtain larger nanocrystals. However, when the amount of oleic acid is merely sufficient to provide ligand stabilization, the reactivity of the Pb monomer will be maximized. Then, the nucleating event can result in a large number of smaller particles. Finally, a large monomer concentration gives to a small critical size in colloidal synthesis, and generates small nanocrystals.

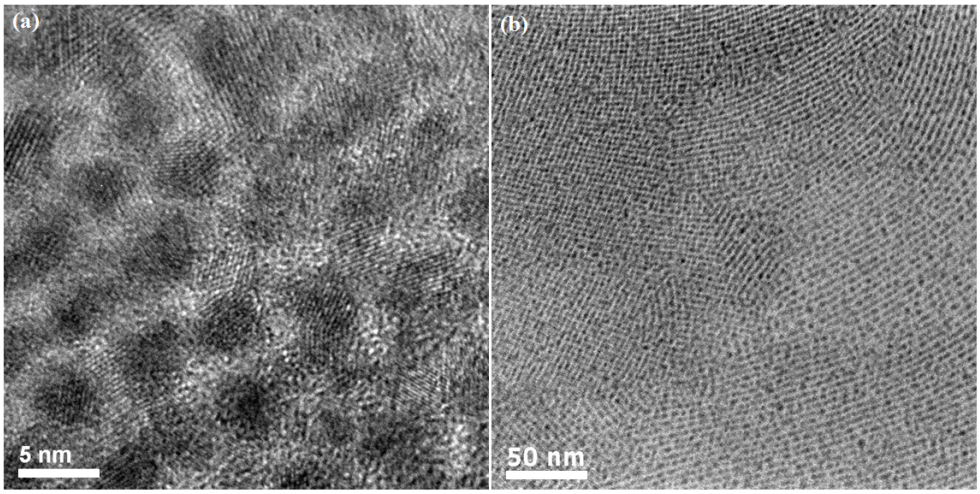

Figure 4.3: (a) PbS nanocrystals with a mean diameter of 4.7 nm synthesized in the presence of excessive OA at low temperature of 80 ^{o}C, with OA:Pb:S = 32:16:1. (b) 2.6 nm PbS nanocrystals synthesized with OA:Pb:S = 4:2:1 at 100 ^{o}C.

4.4 Ligand Exchange

To get rid of the insulating surfactants attached to the nanocrystals, a post synthetic ligand exchange was conducted to replace the eighteen-carbon-atom-chain oleate ligand with eight-carbon-atom-chain octylamine [3]. The nanocrystal solution in toluene was precipitated with methanol, dried and redispersed in an excess of octylamine. The solution was heated at 70 ℃ for 8 h and then was redispersed in a new portion of octylamine after precipitation with dimethyformamide (DMF) and drying. The solution was then left at room temperature for 16h, then was precipitated again and redispersed in toluene. After the ligand exchange, the inter nanocrystal distance is considerably reduced as shown in the high resolution TEM image in Figure 4.5.

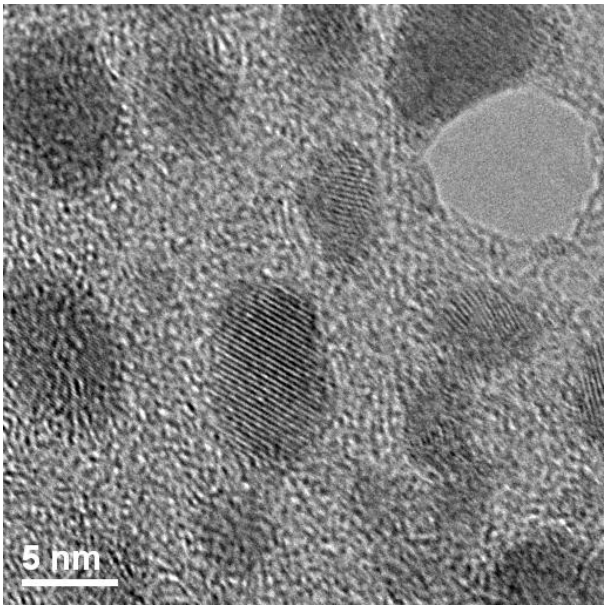

Figure 4.4: HRTEM image of PbS nanocrystals after ligand exchange with octylamine.

4.5 Photo-oxidation and Photoluminescence Enhancement

PbS nanocrystals with bright and narrow photoluminescence as well as sound photo-stability are promising materials for many applications, such as bio-imaging and electroluminescence devices. The photoluminescence of the nanocrystal depends on the surface states, defect in the crystal lattice, and the size of the nanocrystals. Although recent advances in colloidal synthesis have led to the synthesis of small PbS nanocrystals with quantum efficiency as high as 70 %, the corresponding large PbS nanocrystals still have poor quantum efficiency. This contradicts to our intuition and remains not well understood, since smaller nanocrystals should have a larger portion of surface atoms and therefore a greater abundance of surface states. However, the PL of

nanocrystals can be significantly improved through better surface passivation in solution by using surfactants, growing another inorganic shell, or even through photo-oxidation [25, 40].

Surprisingly, a significant PL enhancement is observed for the as synthesized large nanocrystals after exposure to the air, as shown in Figure 4.6. In the classic paper of Hines et al [11], they observed a slight PL increase at the aging process, and they attribute the increase to the size focusing effect. It is the balance between the digestive ripen occurs by large particles breaking apart and smaller particles increasing in size, and an Ostwald ripen process when small particles break apart to feed the growth of large particles until a uniform size distribution is reached [11]. However, in our case, the width of the emission keeps almost the same during the aging process, while PL intensity dramatically increases for more than 2 orders of magnitudes. This dramatic PL increase is way beyond the effect of size focusing, and it was accompanied with an obvious blue shift in the PL energy during a one day period. This indicates the photo-oxidation of the nanocrystals and the formation of outside oxidation layer around the nanocrystal core on the surface. The oxidation layer can protect the semiconductor core and passivate the surface and defect states, which in turn improves the PL of the nanocrystals [40].

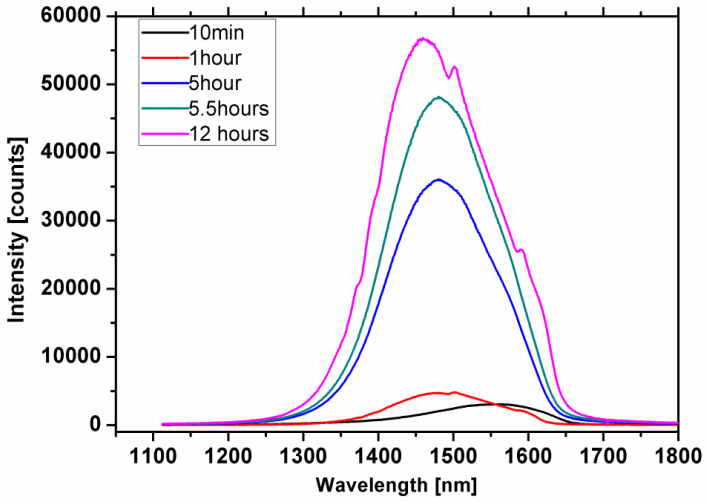

Figure 4.5: PL spectra of PbS nanocrystals after 10 min, 1 hour, 5 hours, 5.5 hours and 12 hours' storage in air.

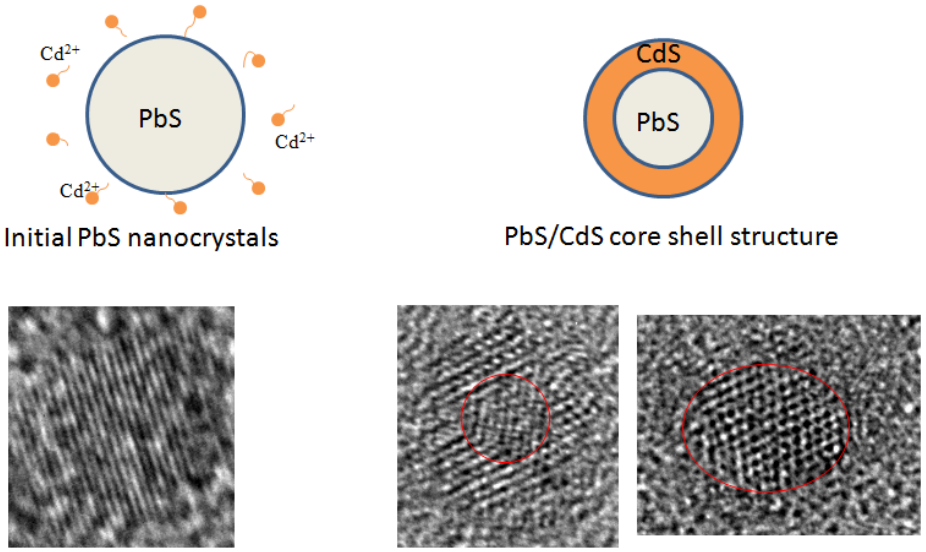

Figure 4.6 : A cartoon showing the formation of CdS shell over PbS nanocrystals.

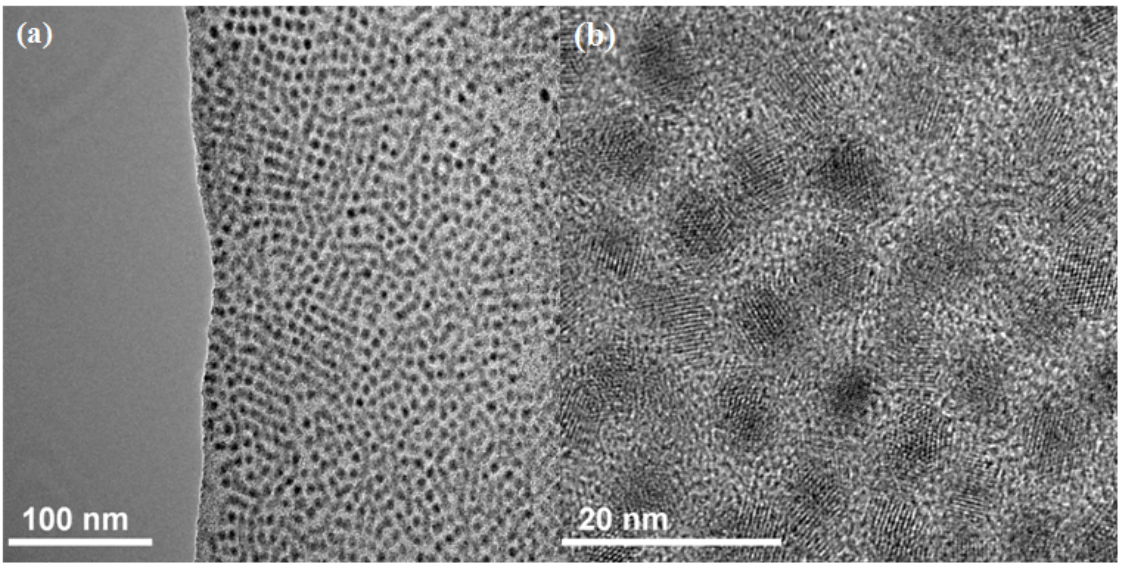

Figure 4.7: (a) TEM and (b) high resolution TEM images showing the PbS/CdS core shell structure.

4.6 PbS/CdS Core Shell Structure

A core shell structure is typically realized through overgrowing a shell of a second semiconductor on the original semiconductor core to improve the NCs' surface passivation. In this manner, the photoluminescence efficiency and stability again photo-oxidation of the nanocrystals can be significantly improved as we have shown previously [41]. Furthermore, it is also possible to tune the emission wavelength in a large spectral window by choosing the appropriate core and shell materials.

It was reported that Cd ions can replace Pb ions on the surface of PbS nanocrystals resulting in PbS/CdS core shell structure [41]. We obtained the PbS/CdS

core shell by treating the as-synthesized PbS solution with the Cd-oleate solution in octadecene at room temperature. The growth of CdS shell is at the expense of consuming Pb on the nanocrystal surface, as shown in the cartoon in Figrue 4.7, thus the size of the nanocrystals will remain the same after the shell growth.

The raw PbS nanocrystal solutions before precipitation are prepared as described earlier. Then, a Cd-OA stock solution was prepared similarly, with 0.514 g CdO and 0.375 OA in 3 mL ODE degassed in vacuum for 10 min and then kept under 250 ^{o}C to obtain a colorless solution. Afterward, the solution was protected under nitrogen and cooled down to room temperature. Then, the Cd-OA solution is mixed with the PbS nanocrystal solution under vigorous stirring. Aliquots samples of nanocrystals are taken out at different intervals of reaction, blended with a mixture solution of toluene and methanol for the precipitation of nanocrystals.

The core-shell structure was examined by the TEM and HRTEM images as shown in Figure 4.6 and Figure 4.7. The significant difference in atomic number between lead and cadmium render the central PbS regions darker owing to stronger electron diffraction. As a result, the difference in contrast shown in Figure 4.8 (a) between the core and surface of the nanocrystal indicates the formation of core-shell structure. Meanwhile, the high resolution image in Figure 4.7 and Figure 4.8 (b)

clearly shows the discontinuous crystalline lattice near the nanocrystal surface, which also confirms the core-shell nanocrystal structures.

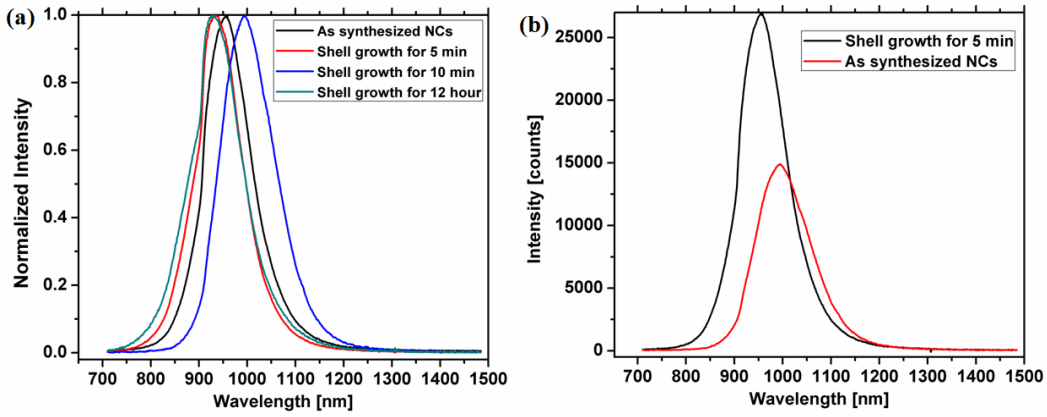

Figure 4.8: (a) The blue shift of PbS nanocrystals after the CdS shell growth for 5 min, 10 min, and 12 hours. (b) The increase PL intensity after the CdS shell growth compare to the original NC.

As shown in Figure 4.9 (a), the nanocrystals exhibits a significant blue shift after the shell growth, indicating the formation of CdS shell and the reduced PbS core size. Even though the original small PbS nanocrystal before shell growth have strong photoluminescence, a significant increase in intensity and a slightly narrowed PL was observed after the shell growth as shown in Figure 4.9. This suggests a better capping with the CdS shell as well as the reduced defect and trap states in the nanocrystal.

4.7 Conclusion

In this chapter, we discussed the controllable synthesis of PbS nanocrystals, the critical point of which lies in a controlled nucleation process, the injection temperature, the molar ratio among the surfactants and precursors, and the monomer concentration. The insulating oleic acid can be replaced by a shorter ligand through ligand exchange in solution. Most importantly, the photoluminescence of PbS nanocrystal can be significantly enhanced by photo-oxidation or by overgrowing an inorganic shell, since the outside oxidation layer and the shell can effectively reduce the surface and defect states in the nanocrystal.

Chapter 5

DIRECTED NANOCRYSTAL SELF-ASSMBLY AND FORMATION OF RADICALLY BRANCHED AND ZIGZAG PBS NANOWIRES

5.1 Introduction

Lead sulfide nanocystals have exhibited many interesting novel size and shape dependent properties. Indeed, strong and symmetric quantum confinement of electrons and holes and large exciton binding energies provide superb quantum efficiencies in high-quality lead-chalcogenide nanostructures [42,44.], translating in highly-efficient band-edge emission and strong photo-response from the mid-infrared down to the ultraviolet [45,46]. Controlling their structural and optoelectronic properties through improved colloidal chemistry remains a very active field of research, which has enabled more complex lead-chalcogenide nanostructures such as nanorods and nanowires [46-51], star-shaped nanocrystals [34, 37,52], nanocubes [34,35], core-shell nanocrystals [41], and octahedral nanocrystals [34,52].

Meanwhile, the self-assembly of lead-chalcogenide nanocrystals into more complex monolayer and film [53-59] structures with a wide range of promising optoelectronic properties has also grown into a very active field of research.

While extensive work has been done with self-assembled nanocrystalline film structures, there are very reports on self-assembled one-dimensional nanocrystalline structrures [28-30]. Even if self-assembled lead-selenide (PbSe) nanowires with different morphologies have been realized using the oriented attachment of nanocrystals [28,29], it was only recently shown that lead-sulfide (PbS) nanowires can also form using this process [30].

In this chapter, we discuss the catalyst-free hot-colloidal synthesis of single-crystal PbS nanowires with different morphologies through the oriented attachment of faceted nanocrystals using multiple surfactants, thus providing high yields of micrometer long nanowires with uniform diameter size distributions. Indeed, we show that the self-attachment of star-shaped nanocrystals can generate radically-branched nanowires, while the assembly of octahedral nanocrystals results in zigzag nanowires. A unique feature of this synthesis consists in a much slower oriented-attachment process compared with the PbSe case previously reported [34]. As such, we demonstrate that this process can provide a much better understanding of the intricacies of this complex nanocrystal assembly method by collecting aliquots at different stages of the reaction. In the future, we believe these unique PbS nanowire morphologies synthesized using facile hot colloidal methods will provide a new level of control to achieve novel low-cost and high-performance light-emitting, photovoltaic and thermoelectric devices.

5.2 PbS Nanowire Synthesis

The synthesis is carried-out inside a nitrogen-purged glove-box. In the glove box, 0.76 g lead acetate trihydrate and 2 ml of oleic acid are added to a single flask and heated to 150°C for around 45 min until the lead acetate dissolved completely and a clear solution was obtained. In a separate flask, 4 ml stock solution of 0.16 M trioctylphosphine sulfide (TOPS) is mixed with 2 ml of oleylamine and 10 ml of octadecene. The sulfur solution is then slowly injected to the hot lead oleate solution at 250 ^{o}C. The reaction solution is maintained at 200 ^{o}C for 1 hour. Then, aliquots of samples were injected into excess amounts of acetone, thereby quenching reaction and the nanowires are precipitated from the solution by centrifugation, dried, and dissolved in toluene or tetrachloroethylene for further characterization and measurement. Smaller nanowires can be synthesized at lower injection (200 ^{o}C) and growth temperature (175 ^{o}C).

5.3 Structural and Morphology of PbS Nanowires

We observed that both an injection and growth temperature higher than 175 ^{o}C is required for the formation of any PbS nanowires using this method. Figure 5.1 shows typical nanowires obtained after reaction at 175 ^{o}C for 1 hour. SEM and TEM micrographs in Figure 5.1(a,b) show an ensemble of 2 to 7 μm-long PbS nanowires with an average diameter of 24 ±3 nm. In Figure 5.1(c), the selected area electron diffraction (SAED) pattern confirms a rock salt-cubic structure with clear {111},

{200}, {220}, and {311} diffraction rings, while the strongest diffraction intensity in the {200} plane suggests a preferred crystalline orientation of the nanowires along the {100} axis. This conclusion is consistent with the high-resolution TEM (HRTEM) observation from multiple nanowires, an example of which is shown in Figure 5.1(d). Finally, the energy dispersive spectroscopy (EDS) analysis shown in Figure 5.1(e) indicates strong Pb and S peaks, while the Cu peak

In contrast, Figure 5.2 shows PbS nanowires obtained after a reaction time of 1 hour using both higher injection (250°C) and growth (200°C) temperatures. Here, the nanowires exhibit strongly-corrugated surface structures with a significantly larger average diameter of 57 nm.

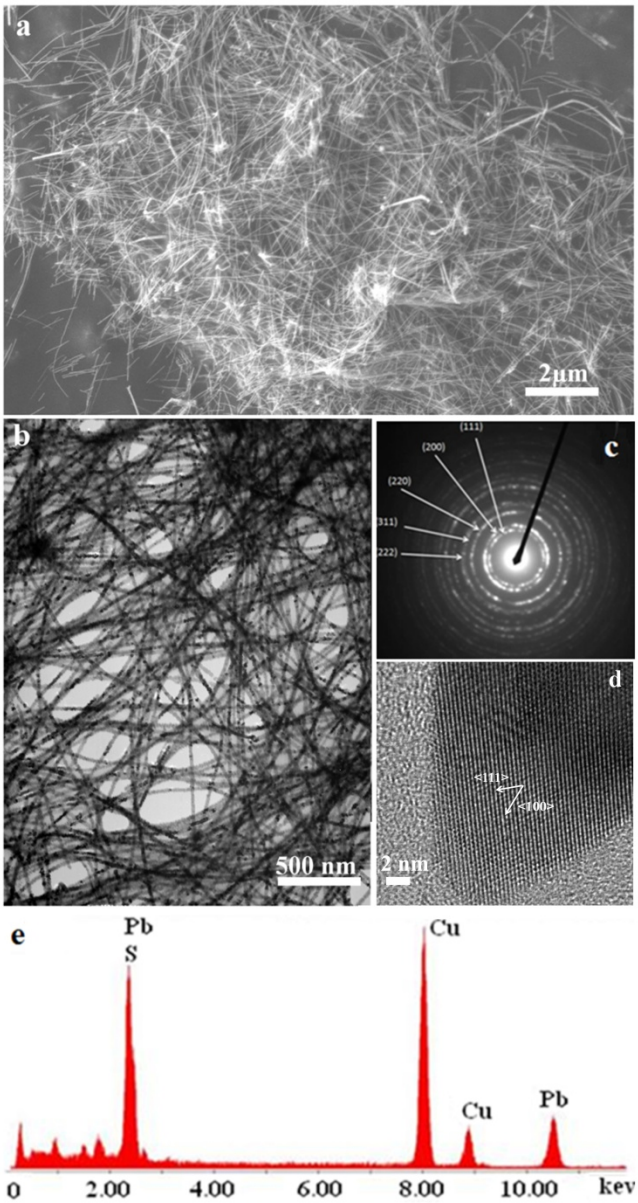

Figure 5.1: Typical PbS nanowires obtained after reaction at 175 ^{o}C for 1 hour. (a) SEM overview. (b) TEM image of a nanowire ensemble showing a uniform 24 ± 3 nm diameter distribution. (c) Selected area electron diffraction rings from the nanowire ensemble in (b). (d) HRTEM image of the end of a typical nanowire imaged along the {111} zone axis and showing the well-defined crystal planes and a selective growth originates from the supporting TEM grid. The overlap of the low-

energy Pb and S peaks prevents confirmation of the exact stoichiometry of the wires.

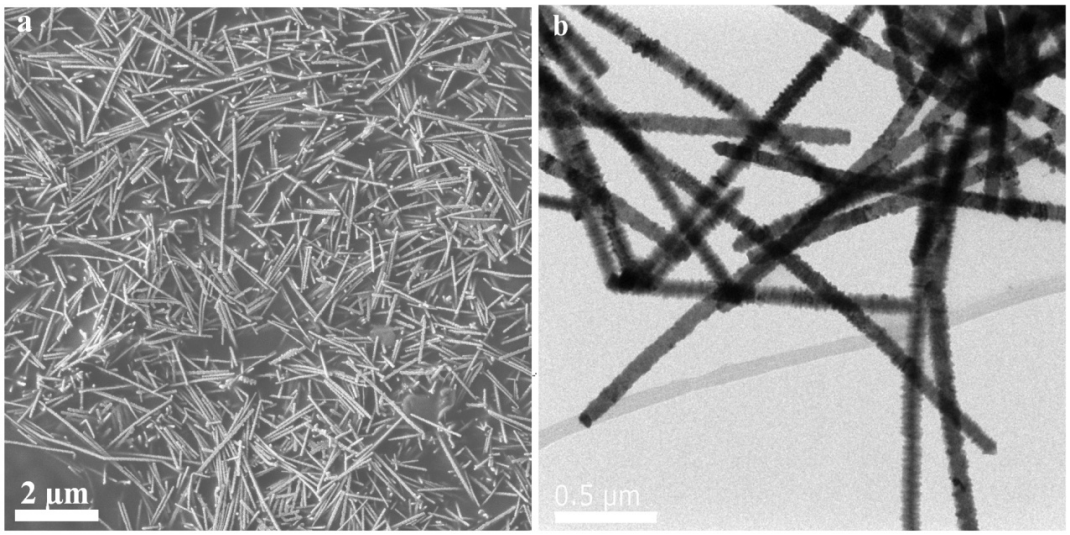

Figure 5.2: Typical PbS nanowires obtained using an injection temperature of 250 ^{o}C and a growth temperature of 200 ^{o}C for 1 hour. (a) SEM overview of PbS nanowires with an average diameter of 57 nm. (b) TEM image showing the corrugated structure of the nanowires.

In Figure 5.3, the structural details of the nanowire morphologies are further examined by HRTEM. It appears that each nanowire displays either a *radically-branched* star-shape structure such as shown in Figure 5.3(a), or a zigzag structure shown in Figure 5.3(b). The HRTEM image in Figure 5.3(a) is taken along the {100} zone axis and clearly shows the lateral structure of a typical star-shape nanowire cross-section. There, both the center region and the sharp side-arms of the nanowire show well-defined lattice fringes of 0.3 nm, corresponding to the {200} direction of the lead-sulfide cubic rock-salt structure. In contrast, the HRTEM image in Figure 5.3(b)

shows a typical zigzag nanowire with well-defined crystal lattice, while the inset clearly shows the quasi-rectangular cross-section of the nanowire. Both the HRTEM images and SAED patterns clearly suggest single-crystal nanowire structures.

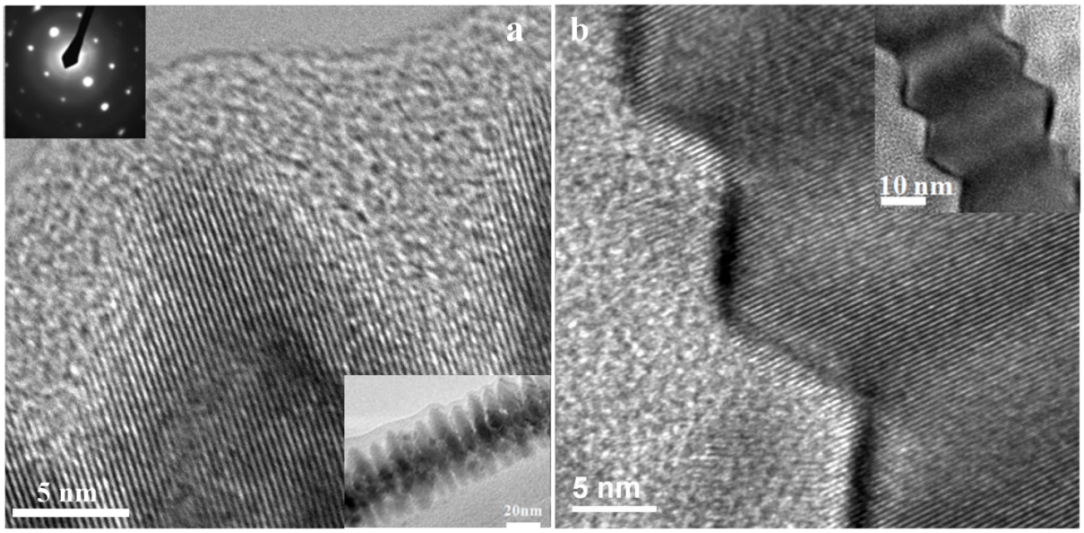

Figure 5.3: High-resolution TEM of radically-branched and zigzag nanowires. (a) HRTEM image showing the lateral structure of the star-shape branched nanowires. The top inset shows the SAED of the single-crystal nanowire, while the lower inset shows the overall morphology of the nanowire at lower resolution. (b) HRTEM image showing the zigzag structure. The inset shows an overall view of the cross section of the nanowire.

In this synthesis process, multiple surfactants can be employed to control the morphologies of the seed nanocrystals. In doing so, different surfactants can interact distinctively with the anions and cations, thus selectively coordinating with the different facets of the nanocrystals and modifying their surface energy during the

reaction. Oleic acid with a COOH- acid group and trioctylphosphine with a phosphine group can bond to Pb sites and the S sites respectively on the surface of the nanocrystals [60]. In a typical cubic cell, the surface energy of the crystallographic facets have a sequence of {111} < {100} < {110} [53]. Introducing the amine in the synthesis can drastically slow down the reaction process by bonding to the positive ions and forming a barrier along the {111} planes [34], whereas the growth along the {100} facets can still proceed owing to its high surface energy [67] If a considerable growth period is allowed, the excessive growth of the {100} facets will produce star-shaped and octahedral nanocrystals. As such, the oleylamine also indirectly plays the key role of triggering the oriented attachment of the nanocrystals into PbS nanowire structures, since the one dimensional growth of the nanowire is driven by the inherent anisotropy of the crystal structure and surface energy, and the dipolar interactions among the nanocrystals [34]. With the {111} growth suppressed, the excessive growth along of the {100} direction results in a strong built-in dipole moment, which eventually becomes strong enough to generate the oriented-attachment of the nanocrystals through dipole-dipole interactions. As the nanowires assemble along the {100} direction, the built-in dipole gets stronger, which in turns accelerate the oriented-attachment process. This model is consistent with our experimental observations, since the reaction solution drastically slows down and remains colorless up to a couple of minutes within the presence of oleylamine. Indeed, this intermediate stage between the injection of the sulfur precursor and the nanocrystal nucleation

enables the reaction solution to reach the dynamic thermal equilibrium, which is ideal for the self attachment of nanocrystals. Because it plays the key role of suppressing the growth of the {111} facets, thus controlling the nanocrystal morphology and introducing the large dipole moment along the {100} axis required to drive the oriented-attachment process, only large nanocube structures can be observed when the exact same reaction is carried out without the oleylamine.

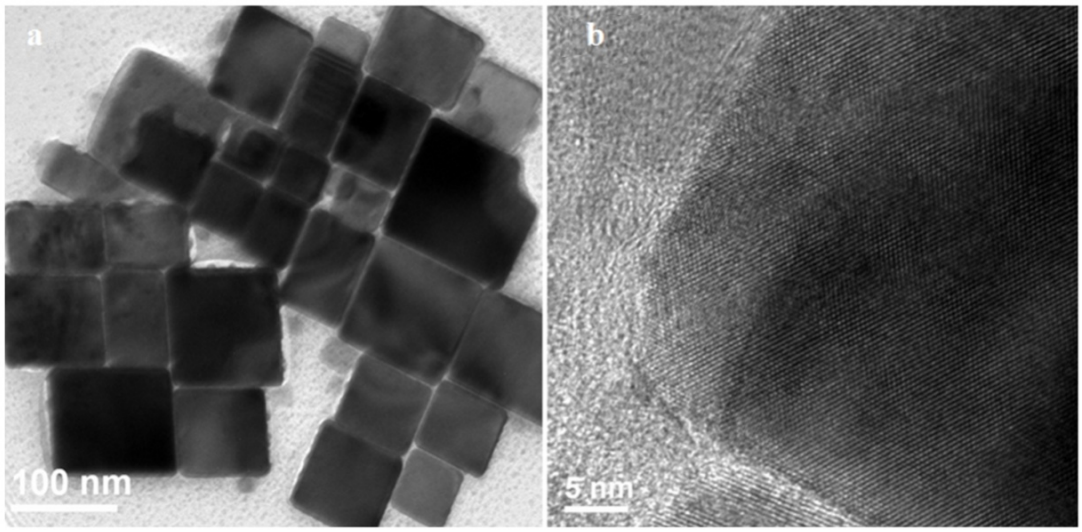

Figure 5.4: The role of oleylamine in the oriented-attachment process. (a) PbS nanocubes obtained from the same reaction as in Figure 5.2, but without the oleylamine. (b) HRTEM image of a typical PbS nanocube.

5.4 Self Assembly and Optical Properties of PbS Nanowires

Although the resulting nanowire morphologies are quite similar to the lead-selenide (PbSe) nanowires previously reported [34,53], the formation mechanism

appears significantly different. In those reports, the initial formation of the PbSe central wire appears to take place within a short period of time at higher injection temperatures, while the growth process proceeds separately and at significantly lower temperatures [34]. In our case, the low reactivity of the partially-inhibitted surfaces leads to a much slower reaction process, which allows a closer examination and more precise control over the formation of the nanowires. Thus, aliquots of samples taken at different intervals during the reaction can be easily collected throughout the reaction and analyzed by SEM, TEM and photoluminescence spectroscopy. While Figure 5.2 shows the final PbS nanowires obtained using an injection temperature of 250 ^{o}C and a growth temperature of 200 ^{o}C for 1 hour, Figure 5.5 (a) shows the low-resolution SEM images of samples collected only 5 minutes and 15 minutes after injection. Mostly nanocrystals with very few nanowires can be observed after 5 minutes. While the sample collected after 15 minutes still consists mainly of small nanocrystal clusters, a larger number of small nanowires can also be observed. As shown in Figure 5.2 and 5.5(b), the oriented-attachment of those small nanoclusters into wires is nearly complete after 60 minutes.

A typical room-temperature absorption and photoluminescence spectra of the primary band-edge emission from the nanowires after the reaction is complete is shown in Figure 5.5 (a). The nanowires exhibit distinct absorption and emission peaks centered at 735 nm and 926 nm respectively. The shift between the absorption peak

and the photoluminescence peak is consistent with the 200-400 meV exciton binding energy expected from PbS nanostructures. The remarkable blue shift from the bulk PbS bandgap suggests a strong quantum confinement located in the side arms and highly-corrugated edges of the nanowires. Other groups observed light emission from PbS nanowires at similar position (655nm, 794nm), and they suggest the emission originates from the multiple single crystal domain in the PbS nanowires [61,62]. This is highly unlikely to be the case here for large quantities of SAED and HRTEM images such as shown in Figure 5.3 have confirmed the single-crystal structure of those self-assembled nanowires. As shown in Figure 5.5 (b), a better insight into the nanocrystal assembly process and the origin of the nanowires' near-infrared emission, can be gained from the photoluminescence spectroscopy of aliquots collected at different stages of the reaction. In the early stage of the reaction, near spherical PbS nanoparticles are formed shortly after the nanocrystal nucleation as shown in figure 5.5 (c), which generates a very weak and broad photoluminescence in the near infrared with peak centered at 1081 nm. As the reaction evolves, the nanoparticles grow along the {100} and {110} facets and form star-shaped and octahedral nanocrystals with long side arms and sharp edges as shown in figure 5.5 (d). Consequently, the sharp emission peak centered at 960 nm emerges rapidly, owing to the strong quantum confinement in the long side arms and sharp edges. Finally, the nanocrystals assemble into nanowires as shown in figure 5.5 (f) and (g), while the strong emission at 960 nm remains as the nanowire maintains the complex morphologies of star shape and

octahedral nanocrystals. This is consistent with our speculation that side arms and highly-faceted edges really dominate the optoelectronic properties of those nanowires. Meanwhile, this also excludes the possibility that the emission originates from the single crystal domains in the PbS nanowires, as it was previously speculated [62].

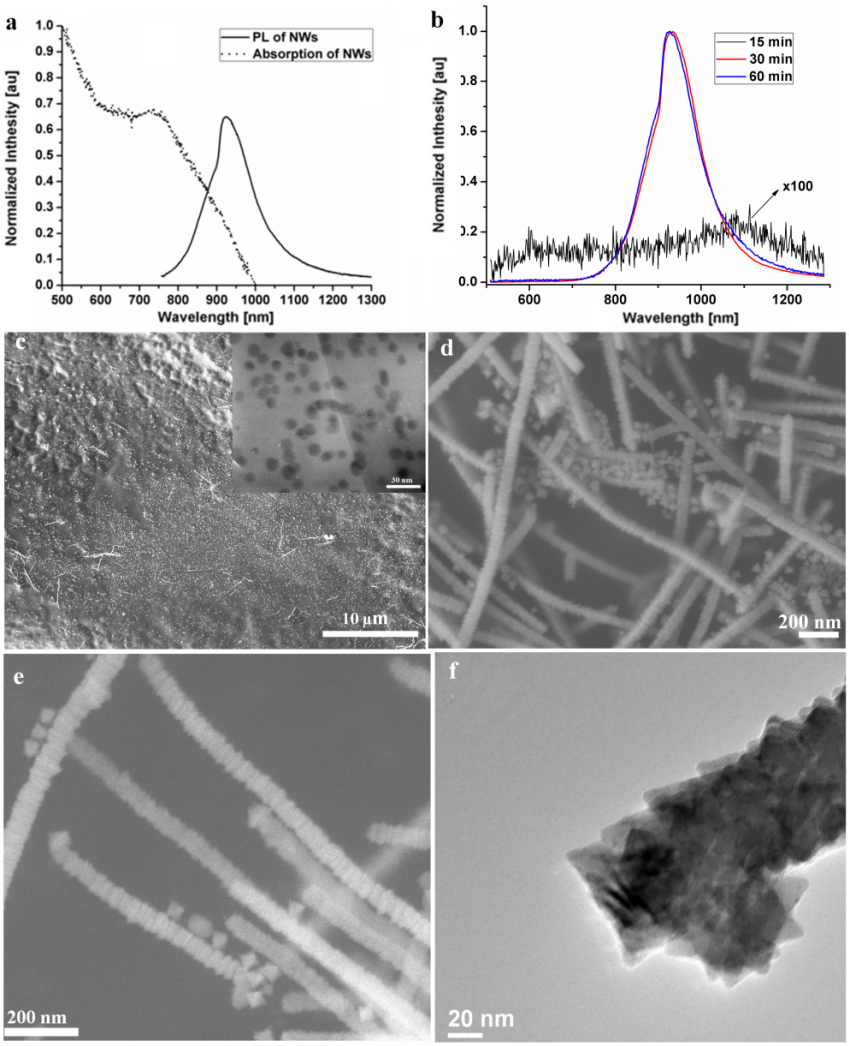

Figure 5.5: Analysis of aliquots collected at different stages of the reaction using an injection temperature of 250 ^{o}C and a growth temperature of 200 ^{o}C. (a) Room temperature, absorption and photoluminescence spectra of the

nanowires collected after 60 minutes. (b) Room temperature photoluminescence spectra of aliquots collected after 15 min, 30 min and 90 min reaction. (d) Low-resolution SEM of aliquot collected 15 minutes after the start of the reaction. The sample consists mostly of small self-assembled nanocrystalline clusters with few nanowires. The TEM inset shows that after 5 minutes of reaction, the sample consists exclusively of small PbS nanocrystals. (e) After 60 minutes, the TEM reveals that the small nanocrystals have evolved into star-shaped and octahedral nanocrystals, while the majority of those nanocrystals have self-attached into nanowires. (f), (g) SEM and TEM image showing the self-attachment of the building blocks (star shape and octahedral PbS nanocrystals) to the tip of the nanowire.

At the reaction's early stages, these results suggest that the majority of the small nucleates are aggregated into larger clusters along the high energy {100} facets to form star shape nanocrystals and octahedrals, while the high reaction temperature allows rearrangement and annealing of the constituent atoms into single-crystal structures. Then, the nanowire growth is driven by the increasing polarizablity and dipole movement along the growing axis as the number of attached nanocrystals is increasing. Consequently, the star-shaped nanocrystals can self-attach along the {100} direction to form branched nanowires, while the octahedrals can assemble along the {001} direction and finally evolve into zigzag nanowires.

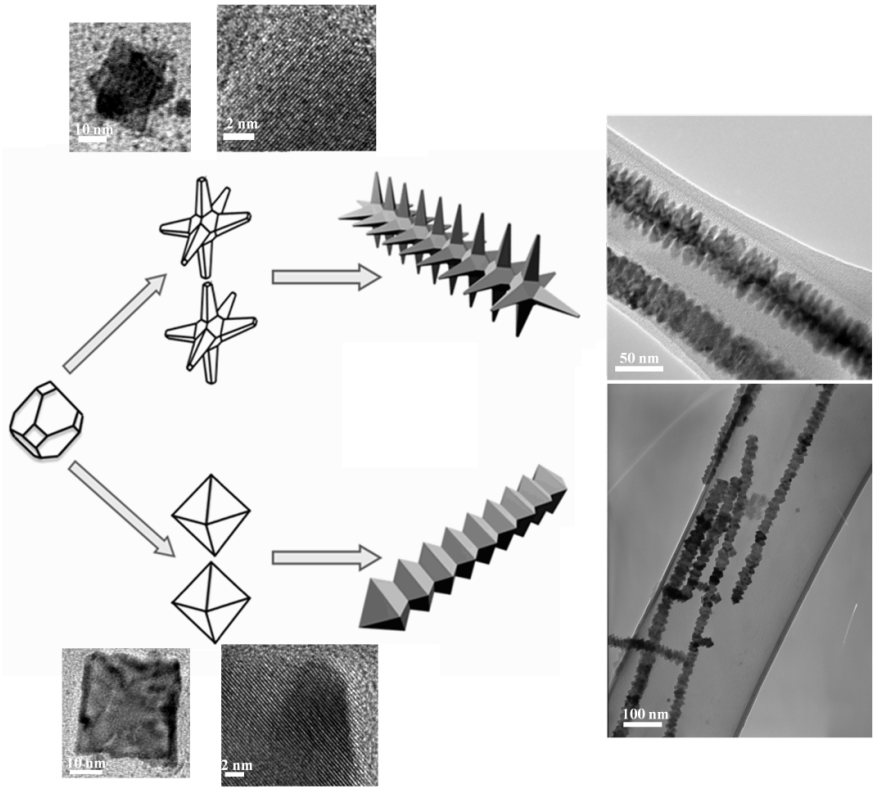

Figure 5.6. Schematic illustration of the nanowire growth process. Shows the evolution from PbS nucleates to star-shaped and octahedral nanocrystals, and the following nanocrystal oriented-attachment process that leads to the formation of-radically branched and zigzag nanowires respectively.

Generally, nanowires can confine carriers in two dimensions, and quantum confinement is not expected when the diameter of the nanowires is larger than the Bohr radius. In the present case, strong quantum confinement can still occur at the narrow side arms of the star-shape branched nanowires or in the highly-faceted sharp edges of the zigzag nanowires albeit their significantly large diameter [52]. Moreover it can be reasonably speculated that the periodic presence of side arms and highly-

faceted edges could potentially be used modulate the band structures of the nanowires to form a one-dimensional mini-band superstructure, with bandgap energy increasing from the thicker inner part to the thinner side-arms and sharper edges. Since the optical properties of nanocrystals are dominated by their lowest dimension [63], these nanowires could also provide an unprecendented level of control over the opto-electronic properties of PbS nanostructures through their unique morphologies.

5.5 Conclusion

In summary, we demonstrate that self-assembly of single-crystal PbS nanowire structures of different morphologies can be achieved using a high-yield hot colloidal method with multiple surfactants. These one-dimensional nanostructures are formed using directed self-assembly of faceted nanocrystals, where the oriented attachment of star shaped nanocrystals leads to radically-branched nanowires while the assembly of octahedral nanocrystals leads to zigzag nanowires. The synthesized nanowires exhibit strong position dependent quantum confinement, which occurs at the side arms and high faceted edges. As a result, the nanowires exhibit strong absorption and fluorescence in the near infrared region and their low reaction speed provides a better understanding of the complex oriented-attachment of nanocrystals into nanowire structures and the exact origin of their near infrared emission. Indeed, these high-quality single-crystal PbS nanowires with unique morphologies and excellent optical properties synthesized using facile hot colloidal methods could become promising

nanomaterials for emerging low-cost and high-performance light-emitting, photovoltaic and thermoelectric devices.

Chapter 6

CONCLUSION

6.1 Thesis Summary

In this chapter, we summarize the major finding of our research. We will discuss the significance of these contributions to the field of PbS nanocrystals, and close with a presentation for our future research.

In chapter 2, we discussed the quantum confinement in PbS nanocrystals using a simplified effective mass approximation and a hyperbolic band model. The effective mass approximation provides a rough estimate of the bandgap of QDs as a function of size. However, this approximation breaks down owing to the nonparabolicity of the band structure at smaller diameter, while the hyperbolic model gives a rather accurate description to the lowest interband optical transition of PbS QDs considering the coupling of the localized valence band state and conduction band state.

The nanocrystals can exhibit different density of states when quantum confinement occurs in different dimensions, giving rise to distinctive opto-electronic

properties when in the form of quantum well, nanowire, and quantum dot. The successful synthesis of PbS nanowires with novel morphologies allows to survey the morphology-dependent quantum confinement. According to the strong photoluminescence in the near infrared region, it can be reasonably speculated that the periodic presence of side arms and highly faceted edges can also modulate the band structures of the nanowires via strong quantum confinement, and with bandgap energy increasing from the thicker inner part to the thinner sidearms and sharper edges.

In chapter 3 and 4, the synthesis of PbS nanocrystals is described. The critical point to control the size of nanocrystals lies in the controlled nucleation process, which is mainly determined by the following three factors: the injection temperature, the molar ratio between the surfactants and precursors, and the monomer concentration. Thermally stable larger nanocrystal can be obtained at higher reaction temperature, while the higher surfactant (such as oleic acid) concentration can lower the monomer reactivity and prevent nanocrystal nucleation. As a result, more monomers can feed to the growth of the nanocrystals, and larger nanocrystals can be synthesized. Finally, larger monomer concentration typically induces a smaller critical size, and generates small nanocrystals.

In chapter 5, we demonstrate that self-assembly of single-crystal PbS nanowire structures of different morphologies can be achieved using a high-yield hot colloidal

method with multiple surfactants. These one-dimensional nanostructures are formed using directed self-assembly of faceted nanocrystals, where the oriented attachment of star shaped nanocrystals leads to radically-branched nanowires while the assembly of octahedral nanocrystals leads to zigzag nanowires. The synthesized nanowires exhibit strong position dependent quantum confinement, which occurs at the side arms and high faceted edges. As a result, the nanowires exhibit strong absorption and fluorescence in the near infrared region and their low reaction speed provides a better understanding of the complex oriented-attachment of nanocrystals into nanowire structures and the exact origin of their near infrared emission. Indeed, these high-quality single-crystal PbS nanowires with unique morphologies and excellent optical properties synthesized using facile hot colloidal methods could become promising nanomaterials for emerging low-cost and high-performance light-emitting, photovoltaic and thermoelectric devices.

6.2 Contributions to the Field

We synthesized various sizes of lead salt nancrystals that exhibit remarkable photoluminescence efficiencies across the near infrared region at room-temperature, which can lead to appealing active material for light emitting devices, photovoltaic devices, and bio-imaging.

In this thesis, we developed the catalyst-free self-attachment of PbS nanowires in hot colloidal solution using a combination of multiple surfactants. We demonstrate that the controllable self-attachment of star-shaped nanocrystals can lead to radically-branched nanowires while the assembly of octahedral nanocrystals leads to zigzag nanowires. The synthesized nanowires exhibit strong position dependent quantum confinement, which occurs at the side arms and high faceted edges of the nanowires. Those novel structures give rise to the appealing optical properties of the nanowires, with strong photoluminescence in the near infrared region.

6.3 Future Works

This successful colloidal synthesis of PbS nanocrystals project has opened many avenues towards the fabrication of various efficient devices, particularly the electroluminescence and photovotalic devices.

In the electroluminescent devices, we plan to use a layer by layer dip-coating to deposit multiple layers of nanocrystals to use as the active layer of new optoelectronic device. Meanwhile, we plan to introduce a well controlled size gradient in multiple layers of NCs to the device to improve the carrier injection. Furthermore, we believe the excitation energy in the surface state of small NCs can be recycled to the excitation state of large NCs, which can in turn increase the efficiency of the devices.

On the other hand, we will try to use the colloidal synthesized PbS/CdS core-shell nanocrystals as the infrared active material, instead of PbS nanocrystals. The CdS shell can form a type I heterojunction with the PbS core and separates the surface of core from the surrounding atmosphere, which can significantly improve the optical fluorescence quantum yield and air stability of the nanocrystals. In the electroluminescent device, such a type I heterojunction can facilitate the carrier injection to the NIR active core and dramatically increase radiative recombination, thus optimizing their efficiencies

For the fabrication of photovoltaic device, we will work on the TiO2-PbS nanocrystal structure, using PbS nanocrystal as the active material hole transporting layer and the TiO2 as the electron acceptor and hole blocking layer.

.

REFERENCES

[1] C. B. Murray, D. J. Norris, and M. G. Bawendi, "Synthesis and characterization of nearly monodisperse CdE (E = sulfur, selenium, tellurium) semiconductor nanocrystallites," Journal of American Chemistry Society 115, 8706–8715 (1993)

[2] M. L. Steigerwald, A. P. Alivisatos, J. M. Gibson, T. D. Harris, R. Kortan, A. J. Muller, A. M. Thayer, T. M. Duncan, D. C. Douglas, and L. E. Brus, "Surface Derivatization and Isolation of Semiconductor Cluster Molecules," Journal of American Chemical Society 110, 3046-3050 (1988)

[3] S.A. Mcdonald, G. Konstantatos, S. Zhang, P. W. Cyr, E. J. D. Klem, L. Levina, and E. D. Sargent, "Solution-processed PbS quantum dot infreared photodetectors and photovoltaics," Nature Materials 4, 138 – 142 (2005)

[4] R. J. Ellingson, M. C. Beard, J. C. Johnson, P. Yu, O. L. Micic, A. J. Nozik, A. Shabaev, and A. L. Afros, "Highly Efficient Multiple Exciton Generation on Colloidal PbSe and PbS Quantum Dots," Nano Letters 5, 865-871 (2005)

[5] S. Günes, K. P. Fritz, H. N. S. Sariciftci, and S. Kumar, and G. D. Scholes, "Hybrid solar cells using PbS nanoparticles," Solar Energy & Solar Cells 91, 420-423, (2007)

[6] S. Coe, W. K. Woo, M. Bawendi, and V. Bulovic, "Electroluminescence from single monolayers of nanocrystals in molecular organic devices," Nature 420, 800-803, (2002)

[7] L. Bakueva, S. Musikhin, M. A. Hines, T.-W. F. Chang, M. Tzolov1, G. D. Scholes, and E. H. Sargent,"Size-tunable infrared (1000-1600nm) electroluminescence from PbS quantum dot nanocrystals in a semiconducting polymer," Applied Physics Letters 82, 2895-3, (2003)

[8] R. C. Somers, M. G. Bawendi, and D. G. Nocera, "CdSe nanocrystal based chem-/bio-sensors," Chemical Society Reviews 36, 579-591 (2007)

[9] H. Rong, R. Jones, A. Liu, O. Cohen, D. Hak, A. Fang, and M. Paniccia, “A continuous-wave raman silicon laser," Nature 433, 725-728 (2005)

[10] K. Müllen and U. Scherf (Eds.), “Organic Light-Emitting Devices: Synthesis, Properties and Applications,” (Wiley-VCH, Weinheim, Germany, 2006).

[11] M. A. Hines and G. D. Scholes, “Colloidal PbS nanocrystals with size-tunable near-infrared emission: observation of post-synthesis self-narrowing of the particle size distribution,” Advanced Materials 15, 1844-1849 (2003)

[12] S. Hoogland, V. Sukhovatkin, I. Howard, S. Cauchi, L. Levina, and E. Sargent, “A solution-processed 1.53 mu m quantum dot laser with temperature-invariant emission wavelength," Optics Express 14, 3273-3281 (2006)

[13] K. N. Bourdakos, D. M. N. M. Dissanayake, T. Lutz, S. R. P. Silva, and R. J. Curry, “Highly efficient near-infrared hybrid organic-inorganic nanocrystal electroluminescence device,” Applied Physics Letters 92, 153311-3 (2008)

[14] P. O. Anikeeva, J. E. Halpert, M. G. Bawendi, and V. Bulovic, “Electroluminescence from a mixed Red-Green-Blue Colloidal Quantum Dot Monolayer,” Nano Letter 7, 2196-2200 (2007)

[15] C. B. Murray and C. R. Kagan, “Synthesis and Characterization of Monodisperse Nanocrystals and Close-Packed Nanocrystal Assemblies,” Annual Review of Materials Science 30, 545-610 (2000)

[16] L. Sun, L. Bao, B.-R. Hyun, A. C. Bartnik, Y.-W. Zhong, J. C. Reed, D.-W. Pang, H. C. Abruna, G. G. Malliaras and F. W. Wise, “Electrogenerated Chemiluminescence from PbS Quantum Dots”, Nano Letters 9, 789-793 (2009)

[17] J. B. Sambur, T. Novet, and B. A. Parkinson, “Multiple Exciton Collection in a Sensitized Photovoltaic System”, Science 330, 63 (2010)

[18] W. A. Tisdale, K. J. Williams, B. A. Timp, D. J. Norris, E. S. Aydil and X.-Y. Zhu, “Hot Electron Transfer from Semiconductor Nanocrystals,” Science 328, 1543-1548 (2010)

[19] G. Konstantatos, C. Huang, L. Levina, Z. Lu, and E. H. Sargent, “Efficient Infrared Electroluminescent Devices Using Solution-Processed Colloidal Quantum Dots,” Advanced Function Materials 15, 1865-1869 (2005)

[20] G. Scholes and G. Rumbles, "Excitons in nanoscale systems," Nature Materials 5, 683-696 (2006)

[21] L. Brus, "Electronic Wave Functions in Semiconductor Clusters: Experiment and Theory," Journal of. Physics Chemistry 90, 2555-2560 (1986)

[22] Y. Wang, A. Suna, W. Mahler, and R. Kasowski, "PbS in polymers. From moleculars to bulk solids," Journal of Chemistry Physics 87, 7315-7322 (1987)

[23] J. H. Davies, "The physics of low-dimensional semiconductors: An introduction," Cambridge University Press (1997)

[24] A. A. Guzelian, "Synthesis and Characterization of III-V Semiconductor Nanocrystals," Dissertation for degree of Doctor of Philosophy, Cornell University, (1996)

[25] K. A. Abel, J. Shan, J. C. Boyer, F. Harris, and F. C. J. M. Van Veggel, "Highly Photoluminescent PbS nanocrystals: The Beneficial Effect of Trioctylphosphine," Chemistry of Materials 20, 3794-3796 (2008)

[26] R. Bose, J. F. McMillan, J. Gao, K. M. Rickey, C. J. Chen. D. V. Talapin, C. B Murray and C. W. Wong, "Temperature Tuning of Near-Infrared Monodisperse Quantum Dot Solids at 1.5 um for Controllable Förster Energy Transfer," Nano Letters 8, 2006-2011 (2008)

[27] W. Lu, I. Kamiya, M. Ichida, and H. Ando, "Temperature dependence of electronic energy transfer in PbS quantum dot films," Applied Physics Letters 95, 08312-3 (2009)

[28] Th. Förster. "Zwischenmolekulare energiewanderung and fluoreszenz," Annalen der Physik 6, 55-75 (1948)

[29] J. J. Choi, J. Luria, B. R. Hyun, A. C. Bartnik, L. Sun, Y. F. Lim, J. A. Marohn, F. W. Wise, and T. Hanrath, "Photogenerated Exciton Dissociation in Highly Coupled Lead Slat Nanocrystal Assemblies," Nano Letters 10, 1805-1811, (2010)

[30] R. A. Marcus, Biochim. N. Sutin, "Electron transfers in Chemistry and biology" Biophysics. Acta 3, 265–322. (1985)

[31] Y. Yin and A. P. Alivisatos, "Colloidal nanocrystal synthesis and the organic-inorganic interface," Nature 437, 664-670 (2005)

[32] C. Schliehe, B. H. Juarez, M. Pelletier, S. Jander, D. Greshnykh, M. Nagel, A. Meyer, S. Foerster, A. Kornowski, C. Klinke, and H. Weller, "Ultrathin PbS Sheets by Two-Dimensional Oriented Attachement," Science 329, 550-553 (2010)

[33] D. V. Talapin and E. V. Shevchenko, "Dipole-Dipole Interactions in Nanoparticles Superlattice," Nano Letters 7, 1213-1219 (2007)

[34] K. S. Cho, D. V. Talapin, W. Gaschler, and C. B. Murray, "Designing PbSe Nanowires and Nanorings through oriented Attachment of Nanoparticles", Journal of American Chemistry Society 127, 7140-7147 (2005)

[35] J. H. Warner and H. Cao, "Shape Control of PbS nanocrystals using multiple surfactants," Nanotechnology 19, 305605-5, (2008)

[36] S. M. Lee, S. N. Cho, and J. Cheon, "Anisotropic Shape Control of Colloidal Inorganic Nanocrystals," Advanced Materials. 5, 441-444 (2003)

[37] Y. Jun, S. M. Kee, N. J. Kang, J. Cheon, "Controlled Synthesis of Multi-armed CdS Nanorod Architectures Using Monosurfactant System," Journal of American Chemistry Society 123, 5150-5151 (2003)

[38] T. Y. Liu, M. Li, J. Ouyang, m. B. Zaman, R. Wang, X. Wu, C.S. Yeh, Q. Lin, B. Yang, and K. Yu, "Non-Injection and Low-Temperature Approach to Colloidal Photoluminescent PbS Nanocrystals with Narrow Bandwidth," Journal of Physical Chemistry C, 113, 2301-2308 (2009)

[39] S. M. Rupich, E. V. Shevchenko, M. I. Bodnarchuk, B. Lee, and D. V. Talapin, "Size-dependent Multiple Twinning in Nanocrystal Superlattices," Journal of American Chemistry Society 132, 289-296 (2010)

[40] T. Zhang, H. Zhao, D. Riabinina, M. Chaker, and D. Ma, "Concentration – Dependent Photoinduced Photoinduced Photoluminescence Enhancement in Colloidal PbS Quantum Dot Solution," Journal of Physical Chemistry C 114, 10153-10159 (2010)

[41] J. M. Pietryga, D. J. Werder, D. J. Williams, J. L. Casson, R. D. Schaller, V. I. Klimov, and J. A. Hollongsworth, "Utilizing the Liability of Lead Selenide to Produce Heterostructured Nanocrysatls with Bright, Stable Infrared Emission," Journal of American Chemistry Society 130, 48879-4885, (2008)

[42] S. Gallardo, M. Gutierrez, A. Henglein, and E. Janata, "Photochemistry and radiation chemistry of colloidal semiconductors - Properties of Q-PbS," Berichte der Bunsengesellschaft für ohysikalishe Chemie 93, 1080-1090 (1989)

[43] J. L. Machol, F. W. Wise, R. C. Patel and D. B. Tanner, "Vibronic quantum beats in PbS microcrystallites," Physical Review B 48, 2819-2822 (1993)

[44] J. P. Yang, S. B. Qadri and B. R. Ratna, "Structural and Morphological Characterization of PbS Nanocrystallites Synthesized in the Bicontinuous Cubic Phase of Lipid," Journal of Physical Chemistry 100, 17255-17259 (1996)

[45] J. M. Pietryga, R. D. Schaller, D. Weder, M. H. Stewart, V. I. Klimov and J. A. Hollingsworth, "Pushing the band gap envelope Mid infrared emitting Colloidal PbSe Quantum dots," Journal of American Chemistry Society 126, 11752 (2004)

[46] S. Acharya, U. K. Gautam, T. Sasaki, Y. Bando, Y. Golan, and K. Aruga, "Ultra Narrow PbS nanorods with Intense Fluorescence," Journal of American Chemistry Society 4594-4595 (2008)

[47] J.-P. Ge, J. Wang, H.-X. Zhang, X. Wang, Q. Peng, and Y.-D. Li, "Orthogonal PbS Nanowire Arrays and Networks and Their Raman Scattering Behavior," Chemistry – A European Journal 11, 1889-1894 (2005)

[48] K.-T. Yong, Y. Sahoo, K. R. Choudhury, M. T. Swihart, J. R. Minter and P. N. Prasad, "Control of the Morphology and Size of PbS Nanowires Using Gold Nanoparticles," Chemistry of Materials 18, 5965-5972 (2006)

[49] F. Zhang and S. S. Wong, "Controlled Synthesis of Semiconducting Metal Sulfide Nanowires," Chemistry of Materials 21, 4541-4554 (2009)

[50] A. Dom, C. R. Wong and M. G. Bawendi, "Electrically Controlled Catalytic Nanowire Growth from Solution," Advanced Materials 21, 3479-3482 (2009)

[51] L. Cademartiri and G. A. Ozin, "Ultrathin Nanowires - A Materials Chemistry Perspective," Advanced. Materials 21, 1013-1020 (2009)

[52] N. Zhao and L. Qi, "Low-Temperature Synthesis of Star-Shaped PbS Nanocrystals in Aqueous Solutions of Mixed Cationic/Anionic Surfactants", Advanced Materials 18, 359-362 (2006)

[53] S. Y. Jang, Y. M. Song, H. S. Kim, Y. J. Cho, Y. S. Seo, G. B. Jung, C.-W. Lee, J. Park, M. Jung, J. Kim, B. Kim, J.-G. Kim and Y.-J. Kim, "Three Synthetic Routes to Single-Crystalline PbS Nanowires with Controlled Growth Direction and Their Electrical Transport Properties", ACS Nano 4, 2391-2401 (2010)

[54] E. J. D. Klem, H. Shukla, S. Hinds, D. D. MacNeil, L. Levina, and E. H. Sargent, "Impact of dithiol treatment and air annealing on the conductivity, mobility, and hole density in PbS colloidal quantum dot solids," Applied Physics Letters 92, 212105-3 (2008)

[55] T. Hanrath, J. J. Choi, and D.-M. Smilgies, "Structure/Processing Relationships of Highly Ordered Lead Salt Nanocrystal Superlattices," ACS Nano 10, 2975-2988 (2009)

[56] J. M. Luther, M. Law, Q. Song, C. L. Perkins, M. C. Beard, and A. J. Nozik, "Structural, Optical, and Electrical Properties of Self-Assembled Films of PbSe Nanocrystals Treated with 1,2-Ethanedithiol," ACS Nano 2, 271-280 (2008)

[57] D. V. Talapin, and C. B. Murray, "PbSe Nanocrystal Solids for n- and p-Channel Thin Film Field-Effect Transistors," Science 310, 86-91 (2005)

[58] E. J. D. Klem, D. D. MacNeil, P. W. Cyr, L. Levina, and E. H. Sargent, "Efficient solution-processed infrared photovoltaic cells: Planarized all-inorganic bulk heterojunction devices via inter-quantum-dot bridging during growth from solution," Applied Physics Letters 90, 183113-3 (2007)

[59] K. K. Nanda and S. N. Sahu, "Self-assembled heterojunction between electrodeposited PbS nanoparticles and indium tin oxide substrate," Applied Physics Letter 79, 2743-2745 (2001)

[60] A. Lobo, T. Möller, M. Nagal, H. Borchert, S. G. Hichey, and H. Weller, "Photoelectron Spectroscopic Investigation of Chemical Bonding in Organically Stabilized PbS nanocrystals," Journal of Physical Chemistry. B 109, 17422-17428 (2005)

[61] C. Li, Y. Zhao, F. Li, Z. Shi, and S. Feng, "Near-Infrared Absorption of Monodisperse Water-Soluble PbS Colloidal Nanocrystal Clusters," Chemistry of Materials 22, 1901-1907 (2010)

[62] J. H. Chen, C. G. Chao, C. J. Ou, T. F. Liu, "Growth and characteristics of lead sulfide nanocrystals produced by the porous alumina membrane," Surface Science 601, 5142-5147 (2007)

[63] K. Nanda and S. N. Dahu, “One-dimensional quantum confinement in electrodeposited PbS nanocrystalline semiconductors,” Advanced Materials 13, 280-283 (2001)

Appendix A

SYNTHESIS OF PBS NANOCRYSTALS AND CAPPING GROUP EXCHANGE

All the synthesis process is done inside a nitrogen purged glove-box. Lead oxide (2 mmol), Octadecene (ODE, 10 ml) and Oleic Acid (OA, 4 mmol) were first added to a single flask. The mixture was heated under in glove-box at 120 ^{o}C until the frothing had subsided and all of the lead oxide (lead acetate) had dissolved. The mixture was then kept at the desired temperature between 70 ^{o}C ~150 ^{o}C. Subsequently, Hexamethyldisilathiane (1mmol) solution diluted by ODE (5 ml) was quickly injected into the reaction flask under vigorously stirring. The color of the reaction solution changes from dark blue to red and finally to black rapidly after the injection of sulfur precursor, indicating a rapid nucleation process. The reaction solution was annealed for 1 min, then the hot plate is unplugged and the reaction solution is slowly cooled down to room temperature. The nanocrystals are finally collected by injection of reaction solution into an organic polar solvent such as methanol, acetone or ethanol for centrifuging. The precipitates were dried in vacuum and redispersed in toluene or chloroform. To ensure adequate removal of the reaction solvents, precipitation and redispersion was repeated again. The nanocrystal solution was finally filtered with 200 nm polytetreafluoroethylene filters.

For ligand exchange, the nanocrystal solution in toluene (50 mg/mL) was dried and dispersed in an excess of octylamine (2 mL). The solution was then heated at 70 ^{o}C for 8 h and precipitated by mixing with excess amount of dimethyformamide (8 mL) and centrifuging. The precipitated nanocrystals was dried under vacuum, redispersed in a new portion of octylamine, and left at room temperature for 16h. Finally, the solution is precipitated with dimethyformamide again, dried under vacuum, and redispersed in toluene.

Appendix B

SYNTHESIS OF PBS/CDS CORE SHELL NANOCRYSTALS

The raw PbS nanocrystal solutions before precipitation are prepare as described in appendix A. Then, a Cd-Oleate stock solution was prepared by adding 0.514 g CdO, 0.375 Oleic Acid, and 3 mL ODE into a flask, the mixture was degassed in vacuum for 10 min and then kept under 250 ^{o}C to obtain a colorless solution. Afterward, the solution was protected under nitrogen and cooled down to room temperature. Then, the Cd-OA solution is mixed with the PbS nanocrystal solution under vigorous stirring at room temperature. Aliquots of sample of nanocrystals are taken out at different intervals of reaction, blended with a mixture solution of toluene and methanol for the precipitation of nanocrystals though centrifuging.

Appendix C

SYNTHESIS OF STAR SHAPE BRANCHED AND ZIGZAG PBS NANOWIRES

The synthesis is carried-out inside a nitrogen-purged glove-box. In the glove box, 0.76 g lead acetate trihydrate and 2 ml of oleic acid are added to a single flask and heated to 150 ^{o}C for around 45 min until the lead acetate dissolved completely and a clear solution was obtained. In a separate flask, 4 ml stock solution of 0.16 M trioctylphosphine sulfide (TOPS) is mixed with 2 ml of oleylamine and 10 ml of octadecene. The sulfur solution is then slowly injected to the hot lead oleate solution at 250 ^{o}C. The reaction solution is maintained at 200 ^{o}C for 1 hour. Then, aliquots of samples were injected into excess amounts of acetone, thereby quenching reaction and the nanowires are precipitated from the solution by centrifugation, dried, and dissolved in toluene or tetrachloroethylene for further characterization and measurement. Smaller nanowires can be synthesized at lower injection (200 ^{o}C) and growth temperature (175 ^{o}C).

Appendix D

PERMISSION LETTERS FOR THE USE OF COPYRIGHTED MATERIALS

AMERICAN CHEMICAL SOCIETY LICENSE TERMS AND CONDITIONS

May 17, 2011

This is a License Agreement between Fan Xu ("You") and American Chemical Society ("American Chemical Society") provided by Copyright Clearance Center ("CCC"). The license consists of your order details, the terms and conditions provided by American Chemical Society, and the payment terms and conditions.

All payments must be made in full to CCC. For payment instructions, please see information listed at the bottom of this form.

License Number	2657170144500
License Date	Apr 27, 2011
Licensed content publisher	American Chemical Society
Licensed content publication	Nano Letters
Licensed content title	Highly Efficient Multiple Exciton Generation in Colloidal PbSe and PbS Quantum Dots
Licensed content author	Randy J. Ellingson et al.
Licensed content date	May 1, 2005
Volume number	5
Issue number	5
Type of Use	Thesis/Dissertation
Requestor type	Not specified
Format	Electronic
Portion	Table/Figure/Micrograph
Number of Table/Figure/Micrographs	1
Author of this ACS article	Yes
Order reference number	4
Title of the thesis / dissertation	THE SYNTHESIS OF PBS NANOCRYSTAL AND THEIR ASSEMBLY INTO COMPLEX NANOWIRE AND NANOCUBE STRUCTURE
Expected completion date	Apr 2011
Estimated size(pages)	75
Billing Type	Invoice
Billing Address	140 Evans hall, university of Delaware Newark, DE 19716 United States
Customer reference info	
Total	**0.00 USD**
Terms and Conditions	

Thesis/Dissertation

ACS / RIGHTSLINK TERMS & CONDITIONS
THESIS/DISSERTATION

INTRODUCTION

The publisher for this copyrighted material is the American Chemical Society. By clicking "accept" in connection with completing this licensing transaction, you agree that the following terms and conditions apply to this transaction (along with the Billing and Payment terms and conditions established by Copyright Clearance Center, Inc. ("CCC"), at the time that you opened your Rightslink account and that are available at any time at <http://myaccount.copyright.com>).

LIMITED LICENSE

Publisher hereby grants to you a non-exclusive license to use this material. Licenses are for one-time use only with a maximum distribution equal to the number that you identified in the licensing process.

GEOGRAPHIC RIGHTS: SCOPE

Licenses may be exercised anywhere in the world.

RESERVATION OF RIGHTS

Publisher reserves all rights not specifically granted in the combination of (i) the license details provided by you and accepted in the course of this licensing transaction, (ii) these terms and conditions and (iii) CCC's Billing and Payment terms and conditions.

PORTION RIGHTS STATEMENT: DISCLAIMER

If you seek to reuse a portion from an ACS publication, it is your responsibility to examine each portion as published to determine whether a credit to, or copyright notice of, a third party owner was published adjacent to the item. You may only obtain permission via Rightslink to use material owned by ACS. Permission to use any material published in an ACS publication, journal, or article which is reprinted with permission of a third party must be obtained from the third party owner. ACS disclaims any responsibility for any use you make of items owned by third parties without their permission.

REVOCATION

The American Chemical Society reserves the right to revoke a license for any reason, including but not limited to advertising and promotional uses of ACS content, third party usage, and incorrect figure source attribution.

LICENSE CONTINGENT ON PAYMENT

While you may exercise the rights licensed immediately upon issuance of the license at the end of the licensing process for the transaction, provided that you have disclosed complete and accurate details of your proposed use, no license is finally effective unless and until full payment is received from you (by CCC) as provided in CCC's Billing and Payment terms and conditions. If full payment is not received on a timely basis, then any license preliminarily granted shall be deemed automatically revoked and shall be void as if never granted. Further, in the event that you breach any of these terms and conditions or any of CCC's Billing and Payment terms and conditions, the license is automatically revoked and shall be void as if never granted. Use of materials as described in a revoked license, as well as any use of the materials beyond the scope of an unrevoked license, may constitute copyright infringement and publisher reserves the right to take any and all action to protect its copyright in the materials.

COPYRIGHT NOTICE: DISCLAIMER

You must include the following copyright and permission notice in connection with any reproduction of the licensed material: "Reprinted (“Adapted” or “in part”) with permission from REFERENCE CITATION. Copyright YEAR American Chemical Society."

WARRANTIES: NONE

Publisher makes no representations or warranties with respect to the licensed material.

INDEMNITY

You hereby indemnify and agree to hold harmless publisher and CCC, and their respective officers, directors, employees and agents, from and against any and all claims arising out of your use of the licensed material other than as specifically authorized pursuant to this license.

NO TRANSFER OF LICENSE

This license is personal to you or your publisher and may not be sublicensed, assigned, or transferred by you to any other person without publisher's written permission.

NO AMENDMENT EXCEPT IN WRITING

This license may not be amended except in a writing signed by both parties (or, in the case of publisher, by CCC on publisher's behalf).

OBJECTION TO CONTRARY TERMS

Publisher hereby objects to any terms contained in any purchase order, acknowledgment, check endorsement or other writing prepared by you, which terms are inconsistent with these terms and conditions or CCC's Billing and Payment terms and conditions. These terms and conditions, together with CCC's Billing and Payment terms and conditions (which are incorporated herein), comprise the entire agreement between you and publisher (and CCC) concerning this licensing transaction. In the event of any conflict between your obligations established by these terms and conditions and those established by CCC's Billing and Payment terms and conditions, these terms and conditions shall control.

JURISDICTION

This license transaction shall be governed by and construed in accordance with the laws of the District of Columbia. You hereby agree to submit to the jurisdiction of the courts located in the District of Columbia for purposes of resolving any disputes that may arise in connection with this licensing transaction.

THESES/DISSERTATION TERMS

Regarding your request for permission to include **your** paper(s) or portions of text from **your** paper(s) in your thesis/dissertation, permission is now automatically granted; please pay special attention to the **implications** paragraph below. The Copyright Subcommittee of the Joint Board/Council Committees on Publications approved the following:

Copyright permission for published and submitted material from theses and dissertations

ACS extends blanket permission to students to include in their theses and dissertations their own articles, or portions thereof, that have been published in ACS journals or submitted to ACS journals for publication, provided that the ACS copyright credit line is noted on the appropriate page(s).

Publishing **implications** of electronic publication of theses and dissertation material

Students and their mentors should be aware that posting of theses and dissertation material on the Web prior to submission of material from that thesis or dissertation to an ACS journal may affect publication in that journal. Whether Web posting is considered prior publication may be evaluated on a case-by-case basis by the journal's editor. If an ACS journal editor considers Web posting to be "prior publication", the paper will not be accepted for publication in that journal. If you intend to submit your unpublished paper to ACS for publication, check with the appropriate editor prior to posting your manuscript electronically.

Reuse/Republication of the Entire Work in Theses or Collections: Authors may reuse all or part of the Submitted, Accepted or Published Work in a thesis or dissertation that the author writes and is required to submit to satisfy the criteria of degree-granting institutions. Such reuse is permitted subject to the ACS' "Ethical Guidelines to Publication of Chemical Research" (http://pubs.acs.org/page/policy/ethics/index.html); the author should secure written confirmation (via letter or email) from the respective ACS journal editor(s) to avoid potential conflicts with journal prior publication*/embargo policies. Appropriate citation of the Published Work must be made. If the thesis or dissertation to be published is in electronic format, a direct link to the Published Work must also be included using the ACS Articles on Request author-directed link - see http://pubs.acs.org/page/policy/articlesonrequest/index.html

* Prior publication policies of ACS journals are posted on the ACS website at http://pubs.acs.org/page/policy/prior/index.html

If your paper has not yet been published by ACS, please print the following credit line on the first page of your article: "Reproduced (or 'Reproduced in part') with permission from [JOURNAL NAME], in press (or 'submitted for publication'). Unpublished work copyright [CURRENT YEAR] American Chemical Society." Include appropriate information.

If your paper has already been published by ACS and you want to include the text or portions of the text in your thesis/dissertation in **print or microfilm formats**, please print the ACS copyright credit line on the first page of your article: "Reproduced (or 'Reproduced in part') with permission from [FULL REFERENCE CITATION.] Copyright [YEAR] American Chemical Society." Include appropriate information.

Submission to a Dissertation Distributor: If you plan to submit your thesis to UMI or to another dissertation distributor, you should not include the unpublished ACS paper in your thesis if the thesis will be disseminated electronically, until ACS has published your paper. After publication of the paper by ACS, you may release the entire thesis (**not the individual ACS article by itself**) for electronic dissemination through the distributor; ACS's copyright credit line should be printed on the first page of the ACS paper.

v1.2

Gratis licenses (referencing $0 in the Total field) are free. Please retain this printable license for your reference. No payment is required.

If you would like to pay for this license now, please remit this license along with your payment made payable to "COPYRIGHT CLEARANCE CENTER" otherwise you will be invoiced within 48 hours of the license date. Payment should be in the form of a check or money order referencing your account number and this invoice number RLNK0. Once you receive your invoice for this order, you may pay your invoice by credit card. Please follow instructions provided at that time.

Make Payment To:
Copyright Clearance Center
Dept 001
P.O. Box 843006
Boston, MA 02284-3006

For suggestions or comments regarding this order, contact Rightslink Customer Support:

THE AMERICAN ASSOCIATION FOR THE ADVANCEMENT OF SCIENCE LICENSE TERMS AND CONDITIONS

May 17, 2011

This is a License Agreement between Fan Xu ("You") and The American Association for the Advancement of Science ("The American Association for the Advancement of Science") provided by Copyright Clearance Center ("CCC"). The license consists of your order details, the terms and conditions provided by The American Association for the Advancement of Science, and the payment terms and conditions.

All payments must be made in full to CCC. For payment instructions, please see information listed at the bottom of this form.

License Number	2657161142910
License date	Apr 27, 2011
Licensed content publisher	The American Association for the Advancement of Science
Licensed content publication	Science
Licensed content title	Hot-Electron Transfer from Semiconductor Nanocrystals
Licensed content author	William A. Tisdale, Kenrick J. Williams, Brooke A. Timp, David J. Norris, Eray S. Aydil, X.-Y. Zhu
Licensed content date	Jun 18, 2010
Volume number	328
Issue number	5985
Type of Use	Thesis / Dissertation
Requestor type	Author of the AAAS published paper
Format	Print and electronic
Portion	Figure
Number of figures/tables	1
Order reference number	
Title of your thesis / dissertation	THE SYNTHESIS OF PBS NANOCRYSTAL AND THEIR ASSEMBLY INTO COMPLEX NANOWIRE AND NANOCUBE STRUCTURE
Expected completion date	Apr 2011
Estimated size(pages)	75
Total	**0.00 USD**

Terms and Conditions

American Association for the Advancement of Science TERMS AND CONDITIONS
Regarding your request, we are pleased to grant you non-exclusive, non-transferable permission, to republish the AAAS material identified above in your work identified above, subject to the terms and conditions herein. We must be contacted for permission for any uses other than those specifically identified in your request above.
The following credit line must be printed along with the AAAS material: "From [Full Reference Citation]. Reprinted with permission from AAAS."
All required credit lines and notices must be visible any time a user accesses any part of the AAAS material and must appear on any printed copies and authorized user might make.
This permission does not apply to figures / photos / artwork or any other content or materials included in your work that are credited to non-AAAS sources. If the requested material is sourced to or references non-AAAS sources, you must

obtain authorization from that source as well before using that material. You agree to hold harmless and indemnify AAAS against any claims arising from your use of any content in your work that is credited to non-AAAS sources.

If the AAAS material covered by this permission was published in Science during the years 1974 - 1994, you must also obtain permission from the author, who may grant or withhold permission, and who may or may not charge a fee if permission is granted. See original article for author's address. This condition does not apply to news articles.

The AAAS material may not be modified or altered except that figures and tables may be modified with permission from the author. Author permission for any such changes must be secured prior to your use.

Whenever possible, we ask that electronic uses of the AAAS material permitted herein include a hyperlink to the original work on AAAS's website (hyperlink may be embedded in the reference citation).

AAAS material reproduced in your work identified herein must not account for more than 30% of the total contents of that work.

AAAS must publish the full paper prior to use of any text.

AAAS material must not imply any endorsement by the American Association for the Advancement of Science.

This permission is not valid for the use of the AAAS and/or Science logos.

AAAS makes no representations or warranties as to the accuracy of any information contained in the AAAS material covered by this permission, including any warranties of
merchantability or fitness for a particular purpose.

If permission fees for this use are waived, please note that AAAS reserves the right to charge for reproduction of this material in the future.

Permission is not valid unless payment is received within sixty (60) days of the issuance of this permission. If payment is not received within this time period then all rights granted herein shall be revoked and this permission will be considered null and void.

In the event of breach of any of the terms and conditions herein or any of CCC's Billing and Payment terms and conditions, all rights granted herein shall be revoked and this permission will be considered null and void.

AAAS reserves the right to terminate this permission and all rights granted herein at its discretion, for any purpose, at any time. In the event that AAAS elects to terminate this permission, you will have no further right to publish, publicly perform, publicly display, distribute or otherwise use any matter in which the AAAS content had been included, and all fees paid hereunder shall be fully refunded to you. Notification of termination will be sent to the contact information as supplied by you during the request process and termination shall be immediate upon sending the notice. Neither AAAS nor CCC shall be liable for any costs, expenses, or damages you may incur as a result of the termination of this permission, beyond the refund noted above.

This Permission may not be amended except by written document signed by both parties.

The terms above are applicable to all permissions granted for the use of AAAS material. Below you will find additional conditions that apply to your particular type of use.

FOR A THESIS OR DISSERTATION

If you are using figure(s)/table(s), permission is granted for use in print and electronic versions of your dissertation or thesis. A full text article may be used in print versions only of a dissertation or thesis.

Permission covers the distribution of your dissertation or thesis on demand by ProQuest / UMI, provided the AAAS material covered by this permission remains in situ.

If you are an Original Author on the AAAS article being reproduced, please refer to your License to Publish for rules on reproducing your paper in a dissertation or thesis.

FOR JOURNALS:

Permission covers both print and electronic versions of your journal article, however the AAAS material may not be used in any manner other than within the context of your article.

FOR BOOKS/TEXTBOOKS:

If this license is to reuse figures/tables, then permission is granted for non-exclusive world rights in all languages in both print and electronic formats (electronic formats are defined below).

If this license is to reuse a text excerpt or a full text article, then permission is granted for non-exclusive world rights in English only. You have the option of securing either print or electronic rights or both, but electronic rights are not automatically granted and do garner additional fees. Permission for translations of text excerpts or full text articles into other languages must be obtained separately.

Licenses granted for use of AAAS material in electronic format books/textbooks are valid only in cases where the electronic version is equivalent to or substitutes for the print version of the book/textbook. The AAAS material reproduced as permitted herein must remain in situ and must not be exploited separately (for example, if permission covers the use of a full text article, the article may not be offered for access or for purchase as a stand-alone unit), except in the case of permitted textbook companions as noted below.

You must include the following notice in any electronic versions, either adjacent to the reprinted AAAS material or in the

terms and conditions for use of your electronic products: "Readers may view, browse, and/or download material for temporary copying purposes only, provided these uses are for noncommercial personal purposes. Except as provided by law, this material may not be further reproduced, distributed, transmitted, modified, adapted, performed, displayed, published, or sold in whole or in part, without prior written permission from the publisher."

If your book is an academic textbook, permission covers the following companions to your textbook, provided such companions are distributed only in conjunction with your textbook at no additional cost to the user:

- Password-protected website
- Instructor's image CD/DVD and/or PowerPoint resource
- Student CD/DVD

All companions must contain instructions to users that the AAAS material may be used for non-commercial, classroom purposes only. Any other uses require the prior written permission from AAAS.

Rights also extend to copies/files of your Work (as described above) that you are required to provide for use by the visually and/or print disabled in compliance with state and federal laws.

This permission only covers a single edition of your work as identified in your request.

FOR NEWSLETTERS:

Permission covers print and/or electronic versions, provided the AAAS material reproduced as permitted herein remains in situ and is not exploited separately (for example, if permission covers the use of a full text article, the article may not be offered for access or for purchase as a stand-alone unit)

FOR ANNUAL REPORTS:

Permission covers print and electronic versions provided the AAAS material reproduced as permitted herein remains in situ and is not exploited separately (for example, if permission covers the use of a full text article, the article may not be offered for access or for purchase as a stand-alone unit)

FOR PROMOTIONAL/MARKETING USES:

Permission covers the use of AAAS material in promotional or marketing pieces such as information packets, media kits, product slide kits, brochures, or flyers limited to a single print run. The AAAS Material may not be used in any manner which implies endorsement or promotion by the American Association for the Advancement of Science (AAAS) or Science of any product or service. AAAS does not permit the reproduction of its name, logo or text on promotional literature.

If permission to use a full text article is permitted, The Science article covered by this permission must not be altered in any way. No additional printing may be set onto an article copy other than the copyright credit line required above. Any alterations must be approved in advance and in writing by AAAS. This includes, but is not limited to, the placement of sponsorship identifiers, trademarks, logos, rubber stamping or self-adhesive stickers onto the article copies. Additionally, article copies must be a freestanding part of any information package (i.e. media kit) into which they are inserted. They may not be physically attached to anything, such as an advertising insert, or have anything attached to them, such as a sample product. Article copies must be easily removable from any kits or informational packages in which they are used. The only exception is that article copies may be inserted into three-ring binders.

FOR CORPORATE INTERNAL USE:

The AAAS material covered by this permission may not be altered in any way. No additional printing may be set onto an article copy other than the required credit line. Any alterations must be approved in advance and in writing by AAAS. This includes, but is not limited to the placement of sponsorship identifiers, trademarks, logos, rubber stamping or self-adhesive stickers onto article copies.

If you are making article copies, copies are restricted to the number indicated in your request and must be distributed only to internal employees for internal use.

If you are using AAAS Material in Presentation Slides, the required credit line must be visible on the slide where the AAAS material will be reprinted

If you are using AAAS Material on a CD, DVD, Flash Drive, or the World Wide Web, you must include the following notice in any electronic versions, either adjacent to the reprinted AAAS material or in the terms and conditions for use of your electronic products: "Readers may view, browse, and/or download material for temporary copying purposes only, provided these uses are for noncommercial personal purposes. Except as provided by law, this material may not be further reproduced, distributed, transmitted, modified, adapted, performed, displayed, published, or sold in whole or in part, without prior written permission from the publisher." Access to any such CD, DVD, Flash Drive or Web page must be restricted to your organization's employees only.

FOR CME COURSE and SCIENTIFIC SOCIETY MEETINGS:

Permission is restricted to the particular Course, Seminar, Conference, or Meeting indicated in your request. If this license covers a text excerpt or a Full Text Article, access to the reprinted AAAS material must be restricted to attendees of your event only (if you have been granted electronic rights for use of a full text article on your website, your website must be password protected, or access restricted so that only attendees can access the content on your site).

If you are using AAAS Material on a CD, DVD, Flash Drive, or the World Wide Web, you must include the following notice in any electronic versions, either adjacent to the reprinted AAAS material or in the terms and conditions for use of your electronic products: "Readers may view, browse, and/or download material for temporary copying purposes only, provided these uses are for noncommercial personal purposes. Except as provided by law, this material may not be further reproduced, distributed, transmitted, modified, adapted, performed, displayed, published, or sold in whole or in part, without prior written permission from the publisher."

FOR POLICY REPORTS:

These rights are granted only to non-profit organizations and/or government agencies. Permission covers print and electronic versions of a report, provided the required credit line appears in both versions and provided the AAAS material reproduced as permitted herein remains in situ and is not exploited separately.

FOR CLASSROOM PHOTOCOPIES:

Permission covers distribution in print copy format only. Article copies must be freestanding and not part of a course pack. They may not be physically attached to anything or have anything attached to them.

FOR COURSEPACKS OR COURSE WEBSITES:

These rights cover use of the AAAS material in one class at one institution. Permission is valid only for a single semester after which the AAAS material must be removed from the Electronic Course website, unless new permission is obtained for an additional semester. If the material is to be distributed online, access must be restricted to students and instructors enrolled in that particular course by some means of password or access control.

FOR WEBSITES:

You must include the following notice in any electronic versions, either adjacent to the reprinted AAAS material or in the terms and conditions for use of your electronic products: "Readers may view, browse, and/or download material for temporary copying purposes only, provided these uses are for noncommercial personal purposes. Except as provided by law, this material may not be further reproduced, distributed, transmitted, modified, adapted, performed, displayed, published, or sold in whole or in part, without prior written permission from the publisher."

Permissions for the use of Full Text articles on third party websites are granted on a case by case basis and only in cases where access to the AAAS Material is restricted by some means of password or access control. Alternately, an E-Print may be purchased through our reprints department (brocheleau@rockwaterinc.com).

REGARDING FULL TEXT ARTICLE USE ON THE WORLD WIDE WEB IF YOU ARE AN ORIGINAL AUTHOR OF A SCIENCE PAPER

If you chose "Original Author" as the Requestor Type, you are warranting that you are one of authors listed on the License Agreement as a "Licensed content author" or that you are acting on that author's behalf to use the Licensed content in a new work that one of the authors listed on the License Agreement as a "Licensed content author" has written.

Original Authors may post the Accepted Version of their full text article on their personal or on their University website and not on any other website. The Accepted Version is the version of the paper accepted for publication by AAAS including changes resulting from peer review but prior to AAASs copy editing and production (in other words not the AAAS published version).

FOR MOVIES / FILM / TELEVISION:

Permission is granted to use, record, film, photograph, and/or tape the AAAS material in connection with your program/film and in any medium your program/film may be shown or heard, including but not limited to broadcast and cable television, radio, print, world wide web, and videocassette.

The required credit line should run in the program/film's end credits.

FOR MUSEUM EXHIBITIONS:

Permission is granted to use the AAAS material as part of a single exhibition for the duration of that exhibit. Permission for use of the material in promotional materials for the exhibit must be cleared separately with AAAS (please contact us at permissions@aaas.org).

FOR TRANSLATIONS:

Translation rights apply only to the language identified in your request summary above.

The following disclaimer must appear with your translation, on the first page of the article, after the credit line: "This translation is not an official translation by AAAS staff, nor is it endorsed by AAAS as accurate. In crucial matters, please refer to the official English-language version originally published by AAAS."

FOR USE ON A COVER:

Permission is granted to use the AAAS material on the cover of a journal issue, newsletter issue, book, textbook, or annual report in print and electronic formats provided the AAAS material reproduced as permitted herein remains in situ and is not exploited separately

By using the AAAS Material identified in your request, you agree to abide by all the terms and conditions herein.

Questions about these terms can be directed to the AAAS Permissions department permissions@aaas.org.

v 2

Gratis licenses (referencing $0 in the Total field) are free. Please retain this printable license for your reference. No payment is required.

If you would like to pay for this license now, please remit this license along with your payment made payable to "COPYRIGHT CLEARANCE CENTER" otherwise you will be invoiced within 48 hours of the license date. Payment should be in the form of a check or money order referencing your account number and this invoice number RLNK0. Once you receive your invoice for this order, you may pay your invoice by credit card. Please follow instructions provided at that time.

Make Payment To:
Copyright Clearance Center
Dept 001
P.O. Box 843006
Boston, MA 02284-3006

For suggestions or comments regarding this order, contact Rightslink Customer Support:
customercare@copyright.com or +1-877-622-5543 (toll free in the US) or +1-978-646-2777.

Fan Xu <xufan@udel.edu>

May I ask for permission to use figure Figure 3 and Figure 4 (a) Advanced Function Materials 15, 1865-1869 (2005) for my master's thesis

3 messages

Fan Xu <xufan@udel.edu> **Wed, Nov 17, 2010 at 12:43 PM**
To: afm@wiley-vch.de

Dear Editor,
I am Fan Xu, a graduate in the universitu of Delaware.

May I ask for permission to use Figure 3 and Figure 4 (a) "Efficient Infrared Electroluminescent Devices Using Solution-Processed Colloidal Quantum Dots," Advanced Function Materials 15, 1865-1869 (2005) for my master's thesis.

Thank you very much.

Best Regards.

Fan Xu

Rights DE <RIGHTS-and-LICENCES@wiley-vch.de> **Thu, Nov 18, 2010 at 5:24 AM**
To: "xufan@udel.edu" <xufan@udel.edu>

Dear Customer,

Thank you for your email.

We hereby grant permission for the requested use expected that due credit is given to the original source.

If material appears within our work with credit to another source, authorisation from that source must be obtained.

Credit must include the following components:

- Books: Author(s)/ Editor(s) Name(s): Title of the Book. Page(s). Publication year. Copyright Wiley-VCH Verlag GmbH & Co. KGaA. Reproduced with permission.
- Journals: Author(s) Name(s): Title of the Article. Name of the Journal. Publication year. Volume. Page(s). Copyright Wiley-VCH Verlag GmbH & Co. KGaA. Reproduced with permission.

With kind regards

Bettina Loycke
****
Bettina Loycke
Senior Rights Manager
Wiley-VCH Verlag GmbH & Co. KGaA
Boschstr. 12

69469 Weinheim
Germany

Phone: +49 (0) 62 01- 606 - 280
Fax: +49 (0) 62 01 - 606 - 332
Email: rights@wiley-vch.de

Von: Fan Xu [xufan@udel.edu]
Gesendet: Mittwoch, 17. November 2010 18:43
An: AFM
Betreff: May I ask for permission to use figure Figure 3 and Figure 4 (a) Advanced Function Materials 15, 1865-1869 (2005) for my master's thesis

[Quoted text hidden]

Fan Xu <xufan@udel.edu> **Tue, May 17, 2011 at 12:35 PM**
To: Luis Gerlein Reyes <gerlein@udel.edu>

[Quoted text hidden]

Fan Xu <xufan@udel.edu>

May I ask permission to use the Figure 3 in Apply Physics Letter 95, 08312-3 (2009) for my master's thesis??

2 messages

Fan Xu <xufan@udel.edu> **Wed, Nov 17, 2010 at 12:52 PM**
To: rights@aip.org

Dear Sir or Madam,

I am Fan Xu, a graduate student in the university of Delaware.

May I ask permission use the Figure 3 in

"Temperature dependence of electronic energy transfer in PbS quantum dot films," Apply Physics Letter 95,

08312-3 (2009)

for my master's thesis?

Thank you very much.

Best Regards

Fan Xu

RIGHTS <Rights@aip.org> **Mon, Nov 29, 2010 at 4:04 PM**
To: Fan Xu <xufan@udel.edu>

Dear Dr. Xu:

Thank you for requesting permission to reproduce material from American Institute of Physics publications.

Permission is granted – subject to the conditions outlined below – for the following:

Figure 3 in
"Temperature dependence of electronic energy transfer in PbS quantum dot films,"
Apply Physics Letter 95, 08312-3 (2009)

To be used in the following manner:

Reproduced in your Master's Thesis for submission to the University of Delaware.

1. The American Institute of Physics grants you the right to reproduce the material indicated above on a one-time, non-exclusive basis, solely for the purpose described. Permission must be requested separately for any future or additional use.

2. This permission pertains only to print use and its electronic equivalent, including CD-ROM or DVD.

3. The following copyright notice must appear with the material (please fill in the information indicated by capital letters): "Reprinted with permission from [FULL CITATION]. Copyright [PUBLICATION YEAR], American Institute of Physics."
Full citation format is as follows: Author names, journal title, Vol. #, Page #, (Year of publication).
For an article, the copyright notice must be printed on the first page of the article or book chapter. For figures, photographs, covers, or tables, the notice may appear with the material, in a footnote, or in the reference list.

4. This permission does not apply to any materials credited to sources other than the copyright holder.

5. If you have not already done so, please attempt to obtain permission from at least one of the authors. The author's address can be obtained from the article.

Please let us know if you have any questions.

Sincerely,
Susann Brailey

~~~~~~~~~~~
Office of the Publisher, Journals and Technical Publications
Rights & Permissions
American Institute of Physics
Suite 1NO1
2 Huntington Quadrangle
Melville, NY 11747-4502
516-576-2268 TEL
516-576-2450 FAX
rights@aip.org

>>> Fan Xu <xufan@udel.edu> 11/17/2010 12:52 PM >>>
[Quoted text hidden]
~~~~~~~~~~~

AMERICAN CHEMICAL SOCIETY LICENSE TERMS AND CONDITIONS

May 17, 2011

This is a License Agreement between Fan Xu ("You") and American Chemical Society ("American Chemical Society") provided by Copyright Clearance Center ("CCC"). The license consists of your order details, the terms and conditions provided by American Chemical Society, and the payment terms and conditions.

All payments must be made in full to CCC. For payment instructions, please see information listed at the bottom of this form.

License Number	2657160145291
License Date	Apr 27, 2011
Licensed content publisher	American Chemical Society
Licensed content publication	Nano Letters
Licensed content title	Photogenerated Exciton Dissociation in Highly Coupled Lead Salt Nanocrystal Assemblies
Licensed content author	Joshua J. Choi et al.
Licensed content date	May 1, 2010
Volume number	10
Issue number	5
Type of Use	Thesis/Dissertation
Requestor type	Not specified
Format	
Portion	Table/Figure/Micrograph
Number of Table/Figure/Micrographs	1
Author of this ACS article	Yes
Order reference number	30
Title of the thesis / dissertation	THE SYNTHESIS OF PBS NANOCRYSTAL AND THEIR ASSEMBLY INTO COMPLEX NANOWIRE AND NANOCUBE STRUCTURE
Expected completion date	Apr 2011
Estimated size(pages)	75
Billing Type	Invoice
Billing Address	140 Evans hall, university of Delaware Newark, DE 19716 United States
Customer reference info	
Total	**0.00 USD**
Terms and Conditions	

Thesis/Dissertation

ACS / RIGHTSLINK TERMS & CONDITIONS
THESIS/DISSERTATION

INTRODUCTION

The publisher for this copyrighted material is the American Chemical Society. By clicking "accept" in connection with completing this licensing transaction, you agree that the following terms and conditions apply to this transaction (along with the Billing and Payment terms and conditions established by Copyright Clearance Center, Inc. ("CCC"), at the time that you opened your Rightslink account and that are available at any time at <http://myaccount.copyright.com>).

LIMITED LICENSE

Publisher hereby grants to you a non-exclusive license to use this material. Licenses are for one-time use only with a maximum distribution equal to the number that you identified in the licensing process.

GEOGRAPHIC RIGHTS: SCOPE

Licenses may be exercised anywhere in the world.

RESERVATION OF RIGHTS

Publisher reserves all rights not specifically granted in the combination of (i) the license details provided by you and accepted in the course of this licensing transaction, (ii) these terms and conditions and (iii) CCC's Billing and Payment terms and conditions.

PORTION RIGHTS STATEMENT: DISCLAIMER

If you seek to reuse a portion from an ACS publication, it is your responsibility to examine each portion as published to determine whether a credit to, or copyright notice of, a third party owner was published adjacent to the item. You may only obtain permission via Rightslink to use material owned by ACS. Permission to use any material published in an ACS publication, journal, or article which is reprinted with permission of a third party must be obtained from the third party owner. ACS disclaims any responsibility for any use you make of items owned by third parties without their permission.

REVOCATION

The American Chemical Society reserves the right to revoke a license for any reason, including but not limited to advertising and promotional uses of ACS content, third party usage, and incorrect figure source attribution.

LICENSE CONTINGENT ON PAYMENT

While you may exercise the rights licensed immediately upon issuance of the license at the end of the licensing process for the transaction, provided that you have disclosed complete and accurate details of your proposed use, no license is finally effective unless and until full payment is received from you (by CCC) as provided in CCC's Billing and Payment terms and conditions. If full payment is not received on a timely basis, then any license preliminarily granted shall be deemed automatically revoked and shall be void as if never granted. Further, in the event that you breach any of these terms and conditions or any of CCC's Billing and Payment terms and conditions, the license is automatically revoked and shall be void as if never granted. Use of materials as described in a revoked license, as well as any use of the materials beyond the scope of an unrevoked license, may constitute copyright infringement and publisher reserves the right to take any and all action to protect its copyright in the materials.

COPYRIGHT NOTICE: DISCLAIMER

You must include the following copyright and permission notice in connection with any reproduction of the licensed material: "Reprinted (“Adapted” or “in part”) with permission from REFERENCE CITATION. Copyright YEAR American Chemical Society."

WARRANTIES: NONE

Publisher makes no representations or warranties with respect to the licensed material.

INDEMNITY

You hereby indemnify and agree to hold harmless publisher and CCC, and their respective officers, directors, employees and agents, from and against any and all claims arising out of your use of the licensed material other than as specifically authorized pursuant to this license.

NO TRANSFER OF LICENSE

This license is personal to you or your publisher and may not be sublicensed, assigned, or transferred by you to any other person without publisher's written permission.

NO AMENDMENT EXCEPT IN WRITING

This license may not be amended except in a writing signed by both parties (or, in the case of publisher, by CCC on publisher's behalf).

OBJECTION TO CONTRARY TERMS

Publisher hereby objects to any terms contained in any purchase order, acknowledgment, check endorsement or other writing prepared by you, which terms are inconsistent with these terms and conditions or CCC's Billing and Payment terms and conditions. These terms and conditions, together with CCC's Billing and Payment terms and conditions (which are incorporated herein), comprise the entire agreement between you and publisher (and CCC) concerning this licensing transaction. In the event of any conflict between your obligations established by these terms and conditions and those established by CCC's Billing and Payment terms and conditions, these terms and conditions shall control.

JURISDICTION

This license transaction shall be governed by and construed in accordance with the laws of the District of Columbia. You hereby agree to submit to the jurisdiction of the courts located in the District of Columbia for purposes of resolving any disputes that may arise in connection with this licensing transaction.

THESES/DISSERTATION TERMS

Regarding your request for permission to include **your** paper(s) or portions of text from **your** paper(s) in your thesis/dissertation, permission is now automatically granted; please pay special attention to the **implications** paragraph below. The Copyright Subcommittee of the Joint Board/Council Committees on Publications approved the following:

Copyright permission for published and submitted material from theses and dissertations

ACS extends blanket permission to students to include in their theses and dissertations their own articles, or portions thereof, that have been published in ACS journals or submitted to ACS journals for publication, provided that the ACS copyright credit line is noted on the appropriate page(s).

Publishing **implications** of electronic publication of theses and dissertation material

Students and their mentors should be aware that posting of theses and dissertation material on the Web prior to submission of material from that thesis or dissertation to an ACS journal may affect publication in that journal. Whether Web posting is considered prior publication may be evaluated on a case-by-case basis by the journal's editor. If an ACS journal editor considers Web posting to be "prior publication", the paper will not be accepted for publication in that journal. If you intend to submit your unpublished paper to ACS for publication, check with the appropriate editor prior to posting your manuscript electronically.

Reuse/Republication of the Entire Work in Theses or Collections: Authors may reuse all or part of the Submitted, Accepted or Published Work in a thesis or dissertation that the author writes and is required to submit to satisfy the criteria of degree-granting institutions. Such reuse is permitted subject to the ACS' "Ethical Guidelines to Publication of Chemical Research" (http://pubs.acs.org/page/policy/ethics/index.html); the author should secure written confirmation (via letter or email) from the respective ACS journal editor(s) to avoid potential conflicts with journal prior publication*/embargo policies. Appropriate citation of the Published Work must be made. If the thesis or dissertation to be published is in electronic format, a direct link to the Published Work must also be included using the ACS Articles on Request author-directed link - see http://pubs.acs.org/page/policy/articlesonrequest/index.html

* Prior publication policies of ACS journals are posted on the ACS website at http://pubs.acs.org/page/policy/prior/index.html

If your paper has not yet been published by ACS, please print the following credit line on the first page of your article: "Reproduced (or 'Reproduced in part') with permission from [JOURNAL NAME], in press (or 'submitted for publication'). Unpublished work copyright [CURRENT YEAR] American Chemical Society." Include appropriate information.

If your paper has already been published by ACS and you want to include the text or portions of the text in your thesis/dissertation in **print or microfilm formats**, please print the ACS copyright credit line on the first page of your article: "Reproduced (or 'Reproduced in part') with permission from [FULL REFERENCE CITATION.] Copyright [YEAR] American Chemical Society." Include appropriate information.

Submission to a Dissertation Distributor: If you plan to submit your thesis to UMI or to another dissertation distributor, you should not include the unpublished ACS paper in your thesis if the thesis will be disseminated electronically, until ACS has published your paper. After publication of the paper by ACS, you may release the entire thesis (**not the individual ACS article by itself**) for electronic dissemination through the distributor; ACS's copyright credit line should be printed on the first page of the ACS paper.

v1.2

Gratis licenses (referencing $0 in the Total field) are free. Please retain this printable license for your reference. No payment is required.

If you would like to pay for this license now, please remit this license along with your payment made payable to "COPYRIGHT CLEARANCE CENTER" otherwise you will be invoiced within 48 hours of the license date. Payment should be in the form of a check or money order referencing your account number and this invoice number RLNK0. Once you receive your invoice for this order, you may pay your invoice by credit card. Please follow instructions provided at that time.

Make Payment To:
Copyright Clearance Center
Dept 001
P.O. Box 843006
Boston, MA 02284-3006

For suggestions or comments regarding this order, contact Rightslink Customer Support:

Fan Xu <xufan@udel.edu>

May I ask for permission to use figure Figure 3 and Figure 4 (a) Advanced Function Materials 15, 1865-1869 (2005) for my master's thesis

2 messages

Fan Xu <xufan@udel.edu> **Wed, Nov 17, 2010 at 12:43 PM**
To: afm@wiley-vch.de

Dear Editor,
I am Fan Xu, a graduate in the universitu of Delaware.

May I ask for permission to use Figure 3 and Figure 4 (a) "Efficient Infrared Electroluminescent Devices Using Solution-Processed Colloidal Quantum Dots," Advanced Function Materials 15, 1865-1869 (2005) for my master's thesis.

Thank you very much.

Best Regards.

Fan Xu

Rights DE <RIGHTS-and-LICENCES@wiley-vch.de> **Thu, Nov 18, 2010 at 5:24 AM**
To: "xufan@udel.edu" <xufan@udel.edu>

Dear Customer,

Thank you for your email.

We hereby grant permission for the requested use expected that due credit is given to the original source.

If material appears within our work with credit to another source, authorisation from that source must be obtained.

Credit must include the following components:

- Books: Author(s)/ Editor(s) Name(s): Title of the Book. Page(s). Publication year. Copyright Wiley-VCH Verlag GmbH & Co. KGaA. Reproduced with permission.
- Journals: Author(s) Name(s): Title of the Article. Name of the Journal. Publication year. Volume. Page(s). Copyright Wiley-VCH Verlag GmbH & Co. KGaA. Reproduced with permission.

With kind regards

Bettina Loycke
****
Bettina Loycke
Senior Rights Manager
Wiley-VCH Verlag GmbH & Co. KGaA
Boschstr. 12

69469 Weinheim
Germany

Phone: +49 (0) 62 01- 606 - 280
Fax: +49 (0) 62 01 - 606 - 332
Email: rights@wiley-vch.de

Von: Fan Xu [xufan@udel.edu]
Gesendet: Mittwoch, 17. November 2010 18:43
An: AFM
Betreff: May I ask for permission to use figure Figure 3 and Figure 4 (a) Advanced Function Materials 15, 1865-1869 (2005) for my master's thesis

[Quoted text hidden]